NON-GAUSSIAN PROPERTIES OF WAVES IN FINITE WATER DEPTH

By

DAVID J. ROBILLARD

DISTRIBUTION STATEMENT A
Approved for public release;
Distribution Unlimited

A THESIS PRESENTED TO THE GRADUATE SCHOOL
OF THE UNIVERSITY OF FLORIDA IN PARTIAL FULFILLMENT
OF THE REQUIREMENTS FOR THE DEGREE OF
MASTER OF ENGINEERING

UNIVERSITY OF FLORIDA

1996

19960919 030

DTIC QUALITY INSPECTED 1

DISCLAIMER NOTICE

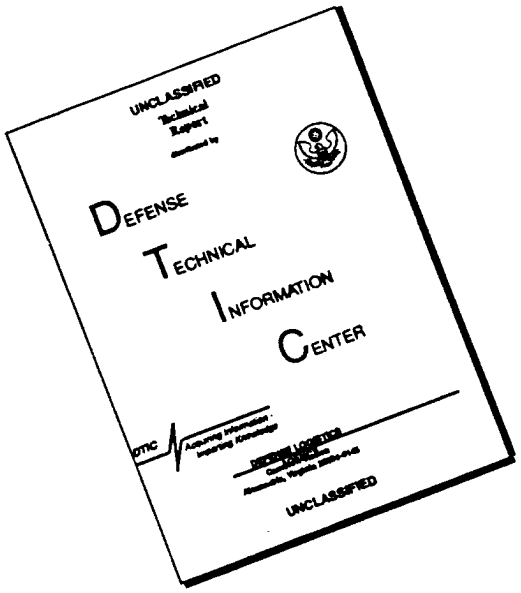

THIS DOCUMENT IS BEST QUALITY AVAILABLE. THE COPY FURNISHED TO DTIC CONTAINED A SIGNIFICANT NUMBER OF PAGES WHICH DO NOT REPRODUCE LEGIBLY.

ACKNOWLEDGMENTS

David J. Robillard wishes to express sincere thanks to his wife and children for their understanding and support. The author would also like to thank the members of the graduate committee, Dr. Michel K. Ochi, Dr. Robert G. Dean and Dr. Ashish Mehta, for their input and guidance during this study. Special thanks are extended to the committee chairman, Dr. Ochi, whose instruction and insight enabled me to learn a great deal on the topic of this study.

TABLE OF CONTENTS

ACKNOWLEDGMENTS ii

LIST OF FIGURES v

LIST OF TABLES viii

ABSTRACT ix

1 INTRODUCTION 1
1.1 Purpose of Study 2

2 LITERATURE REVIEW 5

3 BACKGROUND/STUDY APPROACH 8
3.1 Wave Record Data 8
3.1.1 Data Acquisition 8
3.1.2 Wave Profile Transformations 9
3.2 Nearshore Zone Characteristics 16
3.2.1 Discussion of Water Depth Regions During ARSLOE 16
3.2.2 Discussion of the Surf Zone During ARSLOE 17
3.3 Non-Gaussian Probability Density Function 19
3.3.1 Non-Gaussian Probability Density Function Background 19
3.3.2 Probability Density Function Application to Wave Data 21
3.3.3 Dimensional Analysis of PDF Parameters 22

4 PROBABILITY DENSITY FUNCTION ANALYSIS 24
4.1 Probability Density Function Applicability Verification 24
4.2 Gaussian/Non-Gaussian Boundary Definition 33

5 TREND ANALYSIS OF PARAMETERS 42
5.1 Relationship Between σ and Water Depth 42
5.2 Non-Dimensional PDF Parameter Analysis 44
5.2.1 Spatial Analysis of Data 44
5.2.2 Relationship Between $a\sigma$, μ_*/σ and σ_*/σ 52
5.2.3 Relationship Between $a\sigma$ and σ/d 54

6 SUMMARY AND CONCLUSIONS 56

APPENDIX

COMPARISON OF ORIGINAL AND SMOOTHED "a" VALUES 58

LIST OF REFERENCES 66

BIOGRAPHICAL SKETCH 68

LIST OF FIGURES

Figure page

1.1. Wave Profile Examples: a) Gage 615, Severe Sea Condition, and b) Gage 625, Mild Sea Condition 1

3.1. Coastal Engineering Research Center Field Research Facility 10

3.2. Gage 615 - 10/23 @ 2155 Wave Profile 12

3.3. Gage 635 - 10/23 @ 2155 Wave Profile 12

3.4. Gage 645 - 10/23 @ 2155 Wave Profile 12

3.5. Gage 655 - 10/23 @ 2155 Wave Profile 12

3.6. Gage 665 - 10/23 @ 2155 Wave Profile 13

3.7. Gage 675 - 10/23 @ 2155 Wave Profile 13

3.8. Gage 625 - 10/23 @ 2155 Wave Profile 13

3.9. Gage 615 - 10/25 @ 1315 Wave Profile 14

3.10. Gage 635 - 10/25 @ 1315 Wave Profile 14

3.11. Gage 645 - 10/25 @ 1315 Wave Profile 14

3.12. Gage 655 - 10/25 @ 1315 Wave Profile 14

3.13. Gage 665 - 10/25 @ 1315 Wave Profile 15

3.14. Gage 675 - 10/25 @ 1315 Wave Profile 15

3.15. Gage 625 - 10/25 @ 1315 Wave Profile 15

4.1. Gage 615 - 10/23 @ 2155 Histogram Data 25

4.2. Gage 635 - 10/23 @ 2155 Histogram Data 26

4.3. Gage 645 - 10/23 @ 2155 Histogram Data 26

4.4. Gage 655 - 10/23 @ 2155 Histogram Data 27
4.5. Gage 665 - 10/23 @ 2155 Histogram Data 27
4.6. Gage 675 - 10/23 @ 2155 Histogram Data 28
4.7. Gage 625 - 10/23 @ 2155 Histogram Data 28
4.8. Gage 615 - 10/25 @ 1315 Histogram Data 29
4.9. Gage 635 - 10/25 @ 1315 Histogram Data 29
4.10. Gage 645 - 10/25 @ 1315 Histogram Data 30
4.11. Gage 655 - 10/25 @ 1315 Histogram Data 30
4.12. Gage 665 - 10/25 @ 1315 Histogram Data 31
4.13. Gage 675 - 10/25 @ 1315 Histogram Data 31
4.14. Gage 625 - 10/25 @ 1315 Histogram Data 32
4.15. Sample Data Points to Analyze Gaussian/non-Gaussian Boundary 34
4.16. Probability Density Function of POINT A of Figure 4.15 35
4.17. Probability Density Function of POINT B of Figure 4.15 36
4.18. Probability Density Function of POINT C of Figure 4.15 36
4.19. Probability Density Function of POINT D of Figure 4.15 37
4.20. Probability Density Function of POINT E of Figure 4.15 37
4.21. Probability Density Function of POINT F of Figure 4.15 38
4.22. Probability Density Function of POINT G of Figure 4.15 38
4.23. Probability Density Function of POINT H of Figure 4.15 39
4.24. Gaussian/Non-Gaussian Boundary Defined 41
5.1. Spatial Comparison of σ at Mild and Severe Sea Conditions 43
5.2. Ail σ Data Plotted as a Function of Water Depth 43
5.3. Spatial Comparison of $a\sigma$ at Mild and Severe Sea Conditions 45
5.4. Spatial Comparison of μ_*/σ at Mild and Severe Sea Conditions 46

5.5. Spatial Comparison of σ_*/σ at Mild and Severe Sea Conditions 47

5.6. $a\sigma$ as a Function of Water Depth 49

5.7. μ_*/σ as a Function of Water Depth 50

5.8. σ_*/σ as a Function of Water Depth 51

5.9. Plot of μ_*/σ as a Function of $a\sigma$ for Gages 615 and 625 53

5.10. Plot of σ_*/σ as a Function of $a\sigma$ for Gages 615 and 625 53

5.11. Plot of $a\sigma$ as a Function of σ/d for Mild and Severe Sea Conditions 55

A.1. Plot of Gage 615 Original and Smoothed "a" Values 60

A.2. Plot of Gage 635 Original and Smoothed "a" Values 61

A.3. Plot of Gage 645 Original and Smoothed "a" Values 62

A.4. Plot of Gage 655 Original and Smoothed "a" Values 63

A.5. Plot of Gage 665 Original and Smoothed "a" Values 64

A.6. Plot of Gage 675 Original and Smoothed "a" Values 65

A.7. Plot of Gage 625 Original and Smoothed "a" Values 66

LIST OF TABLES

Table		page
3.1.	Deep Water Wave Statistics for Mild and Severe Sea Conditions	16
3.2.	Surf Zone Locations for Mild and Severe Sea Conditions	19
4.1.	Wave Profile Statistics for Gage 615 - 10/23 @ 2155	25
4.2.	Wave Profile Statistics for Gage 635 - 10/23 @ 2155	26
4.3.	Wave Profile Statistics for Gage 645 - 10/23 @ 2155	26
4.4.	Wave Profile Statistics for Gage 655 - 10/23 @ 2155	27
4.5.	Wave Profile Statistics for Gage 665 - 10/23 @ 2155	27
4.6.	Wave Profile Statistics for Gage 675 - 10/23 @ 2155	28
4.7.	Wave Profile Statistics for Gage 625 - 10/23 @ 2155	28
4.8.	Wave Profile Statistics for Gage 615 - 10/25 @ 1315	29
4.9.	Wave Profile Statistics for Gage 635 - 10/25 @ 1315	29
4.10.	Wave Profile Statistics for Gage 645 - 10/25 @ 1315	30
4.11.	Wave Profile Statistics for Gage 655 - 10/25 @ 1315	30
4.12.	Wave Profile Statistics for Gage 665 - 10/25 @ 1315	31
4.13.	Wave Profile Statistics for Gage 675 - 10/25 @ 1315	31
4.14.	Wave Profile Statistics for Gage 625 - 10/25 @ 1315	32
4.15.	Statistical Properties of Data Points A-H in Figure 4.15	35
5.1.	General Shallow Water Limits of Parameters	52

Abstract of Thesis Presented to the Graduate School
of the University of Florida in Partial Fulfillment of the
Requirements for the Degree of Master of Engineering

NON-GAUSSIAN PROPERTIES OF WAVES IN FINITE WATER DEPTH

By

David J. Robillard

May 1996

Chairman: Michel K. Ochi
Major Department: Coastal and Oceanographic Engineering

As waves propagate into shallower waters, their profile changes from a Gaussian distribution to an increasingly non-Gaussian profile. The non-Gaussian properties of waves in finite water depths are analyzed through the use of a probability density function defined in closed form and that can be solved by the application of wave displacement data. Initially, the applicability of the probability density function is verified using wave data records obtained from the Coastal Engineering Research Center (CERC) at Duck, North Carolina. A broad range of sea conditions and water depths are represented to ensure the probability density function correlates well with actual histogram data over varied conditions. With the applicability verified, the probability density function is used to define criteria for the boundary where the wave field can no longer be considered Gaussian. The ability to determine when a shoaling wave profile can no longer be considered Gaussian is of paramount importance in order to ensure proper wave theories are being applied. This boundary between Gaussian and non-Gaussian wave profiles will be determined in terms of significant wave height and water depth.

Presently, wave data records are required to define the probability density function used in this study. Trend analyses were conducted on the parameters of the probability density function to determine if simplifications can be made to its form and to see if it is possible to define the probability density function in terms of the local conditions, sea severity and water depth, without the need for wave data records.

CHAPTER 1
INTRODUCTION

As wind generated waves transition from deep water to shallow water, a significant change is evident in the wave profile. As an example, Figure 1-1 shows portions of wave records obtained by the Coastal Engineering Research Center, (CERC), during the ARSLOE Project. Figure 1-1(a) is the wave profile recorded at a distance of 60 meters offshore in a shallow intermediate water depth condition. Figure 1-1 (b) is the wave profile taken at the same time but at a distance of 12 km offshore in a deep water condition. Deep water wave profiles in the sea characteristically reflect a Gaussian (linear) random process. The height of the wave crests are probabilistically equal to the height of the wave troughs. As waves move from deep to shallow water, the wave profile transforms from a Gaussian random process to a non-Gaussian (nonlinear) random process in which the wave profile shows a definite excess of high crests and shallow troughs.

a) Gage 615, Severe Sea Condition **b) Gage 625, Mild Sea Condition**

Figure 1.1 Wave Profile Examples

This remarkable transformation in the wave profile, as an irregular sea transitions from deep to shallow water, has also been evidenced in laboratory experiments (Doering and Donelan 1993). The transformation of wave profiles can be attributed to the non-linear wave-wave interactions augmented primarily by decreasing water depth. The "degree" of non-linearity a wave field has at a particular site of interest in the coastal region appears to depend largely on sea severity and water depth.

Although there has been awareness that Gaussian-based solutions do not always represent accurate results in the coastal region, clarification of wave characteristics from deep to shallow water has been a subject of considerable interest in ocean and coastal engineering. There have been few studies which have offered non-Gaussian solutions describing the probability density function of waves in coastal regions. A commonly known study was by Longuet-Higgins (1963), which statistically predicts coastal wave properties using a power series expansion. This probability distribution is based essentially on the Gram-Charlier series distribution. A probability density function developed by Ochi and Ahn (1994a) appears to be applicable throughout the coastal region from deep to shallow water and is defined in closed form Equation (1).

$$f(x) = \frac{1}{\sqrt{2\pi}\sigma_*}\exp\left[-\frac{1}{2(\gamma a\sigma_*)^2}(1-\gamma a\mu_* - \exp(-\gamma a x))^2 - \gamma a x\right] \qquad (1)$$

$$\text{where, } \gamma = \begin{cases} 1.28 \, for: x \geq 0 \\ 3.00 \, for: x < 0 \end{cases}.$$

This is the probability density function that will be used as the basis to analyze coastal wave profiles for this study.

1.1 Purpose of the Study

The overall objective of this study involves two components. The first component will be to validate the applicability of the probability density function developed for waves in finite water depth (Ochi and Ahn 1994a) and to analyze the transition point where wave

profiles can no longer be considered Gaussian. In order to accomplish the first objective of this study, a statistical analysis was carried out on wave time histories obtained during a storm by the Coastal Engineering Research Center (CERC) during the Atlantic Ocean Remote Sensing Land-Ocean Experiment (ARSLOE) Project in 1980. To interpret the transformation of waves from a Gaussian to a non-Gaussian random process, wave records at seven locations were taken where the water depths ranged from two meters to twenty-one meters. In total, approximately 1000 wave records were analyzed with each wave record consisting of 4800 water displacement measurements. The individual wave displacement measurements were recorded at a frequency of 4 Hertz in twenty minute intervals.

Upon confirmation of the probability density functions' applicability, the histogram data will be compared closely with the corresponding normal distribution to determine the conditions under which the wave profile can no longer be considered Gaussian. In particular, general relationships to sea severity and water depth will be determined. A criteria will be established which will define the limit to when the Gaussian wave profile becomes non-Gaussian. This limit will be based on the nonlinearity parameters analyzed from the wave profile data. The second objective of the study will then be to analyze the parameters of the probability density function. The three parameters, a, μ_* and σ_* will be statistically analyzed in both dimensional and non-dimensional form. Trends based on the analysis will be described and relationships linking these parameters of the probability density function to site conditions will be developed.

This study consists of six chapters. Chapter 2 provides a general review on the development of probability density functions applicable to coastal regions. Chapter 3 describes the ARSLOE Project of 1980 and addresses the statistical approach taken in this study. The data used as the basis for this study, were obtained from the ARSLOE Project. This chapter will also describe the local field conditions at CERC during the time the data were collected. Chapter 4 addresses the probability density function applicability and

analysis. This chapter has two distinct sections. The first section reviews the finite water depth probability density function (Ochi and Ahn 1994b) and verifies the applicability of the probability density function. The second section discusses sea severity and water depth and the transition between Gaussian and non-Gaussian wave profiles. Chapter 5 relates the non-dimensionalized parameters of the probability density function, $a\sigma$, μ_*/σ and σ_*/σ, to sea severity, (σ), and water depth in both dimensional and non-dimensional form. The parameters will also be compared to each other and relationships determined. This chapter describes trends evident based on statistical analysis. These trends are qualitative and are intended to give a better understanding of the interaction the wave profile has with its environment as it propagates in shallow waters. Finally, Chapter 6 provides the summary and conclusion for this study.

CHAPTER 2
LITERATURE REVIEW

As stated in the Introduction, the profile of waves in finite water depths is quite different from that observed in deep water. From the stochastic view point, waves in finite water depth are categorized as a non-Gaussian random process for which a precise description of the process does not exist. This is in contrast to the Gaussian random process which can be defined by a rigorous mathematical formulation. Although considerable attention has been given to Gaussian waves in deep water, little information is available on the non-Gaussian characteristics of shallow water waves.

One of the most commonly known presentations describing non-Gaussian waves is the Gram-Charlier series probability density function. This density function is given in a series consisting of an infinite number of terms. Longuet-Higgins (1963) theoretically showed that the statistical properties of nonlinear waves can be presented by the Gram-Charlier series distribution. Bitner (1980) found reasonable agreement in a comparison between the Gram-Charlier series distribution and the histogram constructed from wave data obtained in a relatively shallow water area.

On the other hand, Ochi and Wang (1984) analyzed more than 500 wave records obtained by the Coastal Engineering Research Center (CERC) at Duck, North Carolina during the ARSLOE Project (1980). They found that while the statistical properties of waves at any water depth can be well represented by the Gram-Charlier series distribution, there is a drawback to applying this density function in practice. The probability density function becomes negative for large negative wave displacements and this negative portion does not vanish with increasing number of terms in the series distribution. Because of this

difficulty, the transition property of wave characteristics from gaussian to non-gaussian distribution can not be well clarified. They derived, however, a limiting sea severity for a specified water depth below which wind-generated coastal waves may be considered to be a Gaussian random process.

Another approach for describing the surface elevation of non-Gaussian random waves is to assume that individual waves can be expressed as a Stokes wave. There appears to be some reservation to applying this approach for representing the statistical distribution of the wave profile. This method presupposes a preliminary form of the wave profile before establishing its probability density. This supposition may impose unfavorable bias on the outcome.

Tayfun (1980) derived the probability density function based on the Stokes profile approximation up to the second order. Huang et al. (1983) developed the probability density function considering all terms up to the third order. These probability density functions are superior to the Gram-Charlier series distribution in that they do not have any negative portion over the entire range of wave displacement. Comparison of these probability density functions and wave data show good agreement.

Langley (1987) applied a probability density function representing the response of a non-linear system developed by Kac and Siegert (1947), to nonlinear random waves. This probability density function is given in the form of a series and can only be evaluated numerically. Ochi and Ahn (1994a) modified the Kac Siegert density function so that it is presented in closed form with parameters determined through spectral analysis. They applied the probability density function to non-Gaussian coastal waves. In the application process, they decomposed the spectra into linear and nonlinear components to clarify the degree of non-linearity involved in shallow water waves (Ochi and Ahn 1994b). The probability density function does not have any negative portion in its entire domain and appears to represent the statistical distribution of the wave profile in any sea state during a storm in deep, intermediate and shallow water.

Studies concerned with the non-Gaussian properties of waves in finite water depth include Thornton and Guza (1983) who claimed that the results of their analysis of field data obtained at Torrey Pines Beach, California, show that the Rayleigh probability distribution can be applied to represent wave heights observed from shallow to deep (10.8 meter) water. This implies that all observed waves can be considered a Gaussian random process. However, the sea severity in relation to water depth at all locations in the nearshore zone where their measurements were taken was too mild and below the limit for waves to be a non-Gaussian random process. This subject will be discussed in detail in this present study.

In closing this chapter, it is important to note that there still remains a significant amount of work to do in refining our ability to accurately describe irregular seas in finite water depths and over a wide range of sea severity.

CHAPTER 3
BACKGROUND / STUDY APPROACH

3.1 Wave Record Data

An experiment jointly hosted by the U.S. Army Coastal Engineering Research Center (CERC) and the National Ocean Survey (NOS) was conducted from 06 October 1980 to 30 November 1980. An aspect of this Atlantic Ocean Remote Sensing Land-Ocean Experiment (ARSLOE) involved ocean wave studies implemented near the CERC's Field Research Facility (FRF) at Duck, North Carolina. In situ wave measuring devices were deployed in mean water depths ranging from 1.35 meters to 24.4 meters and were placed in a linear array extending from 60 meters offshore to 12,000 meters offshore, Figure 3.1.

3.1.1 Data Acquisition

The wave displacement data analyzed in this study came from a total of eight wave measuring devices. The FRF has a 550 meter research pier oriented perpendicular to the local shore which was equipped with seven Baylor resistance-type wave staffs. These Baylor wave staffs function by determining the change in electrical resistance experienced by changes in water elevations. Round-trip travel time of an electrical current from an above-water emitter to the water surface is measured. Following along the line of the pier off-shore was a Waverider Buoy Gauge. This is a surface-following class buoy. It functions by double-integrating the output of an accelerometer held vertical by a pendulum to produce the time history of buoy heave motion. The statistics of the buoy heave then represent the wave displacements. In the Waverider buoy, the pendulum is contained

entirely within the spherical float so the buoy does not have to be stabilized. These devices recorded both wave displacements and wave periods but only the displacement data were analyzed for this study. The wave gauges recorded water surface fluctuations simultaneously at all eight locations at a frequency of 4 Hertz over twenty minute intervals. This resulted in 4800 individual wave displacements recorded for each twenty minute segments continuously. Due to the significant amount of data obtained during this unique experiment, only a sub-set of the data was analyzed. This chosen data sub-set began at 1200 on 23 October 1980 and ended at 1315 on 25 October 1980. This two day segment was unique in that a severe storm occurred from 23-25 October which was the most significant meteorological event recorded during the experiment. Wind speeds on the order of fifteen meters per second were recorded during the severe storm. This two day sub-set of data was used as the basis for this study since it included the entire range of wave profiles experienced at each of the eight wave gauge locations. From this two day sub-set, a total of nearly 5 million individual wave displacements were analyzed and the wave profile data covered the entire range of sea conditions present during the complete 56 day ARSLOE Project.

3.1.2 Wave Profile Transformations

The data collected at the FRF during ARSLOE is unique and impressive. It is very well suited for analyzing changes in the wave field as the waves propagate through shoaling depths. The bathymetry at the experiment location is relatively simple showing straight and parallel contours. This provided favorable conditions which maximized control over the environmental impact on the quality of the data received. The wave profile data provide a matrix of wave profiles allowing both spatial and temporal analyses to be performed.

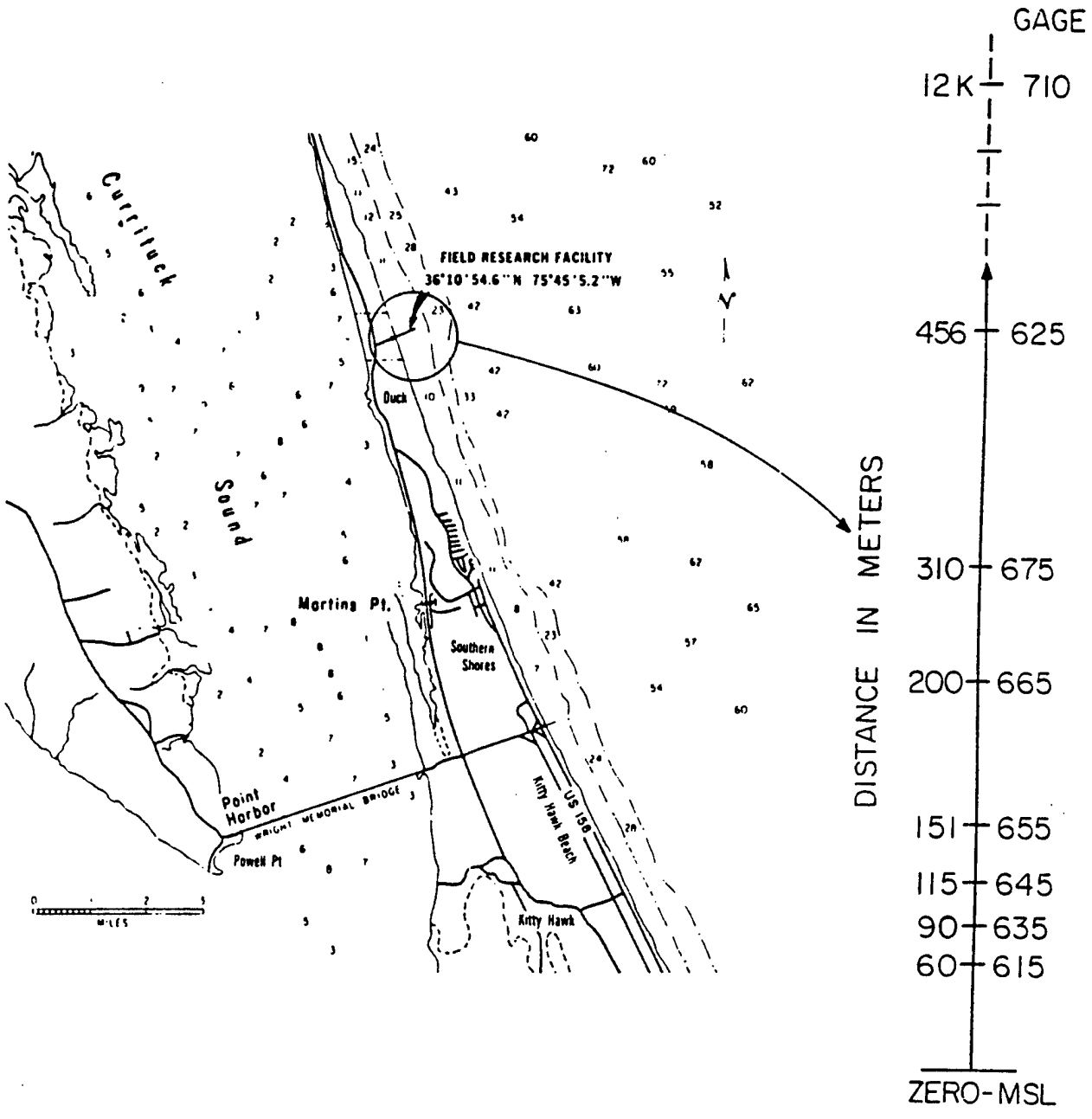

Figure 3.1 Coastal Engineering Research Center Field Research Facility

A wide range of wave profiles was observed during the experiment. Figures 3.2-3.8 represent a mild sea condition recorded on 10/23 @ 2155 for all finite water depth gage locations shown in Figure 3.1. Figures 3.9-3.15 represent a severe sea condition recorded at the height of a storm on 10/25 @ 1315 for the same gage locations. It is evident from the sample wave data that the wave field transitions as it shoals from deep to shallow water. The wave data representing the mild sea condition at Gage 625, Figure 3.8, are characterized by an almost symmetrical distribution of positive and negative wave profile displacements. This is characteristic of Gaussian random processes. As the wave shoals into shallower water, the wave profile transforms showing progressively higher peaks and shallower troughs. This process is clearly non-Gaussian and must be analyzed differently. It is also clear from observing these wave records that the degree of non-linearity increases as the relative water depth decreases and as sea severity increases. This implies that analysis of this nonlinearity must include a dependence on water depth as it relates to the magnitude of the waves' displacement (sea severity).

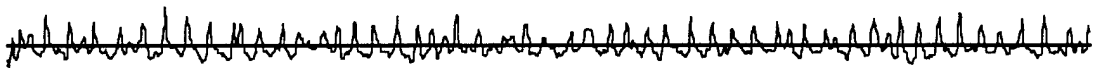

Figure 3-2 Gage 615 - 10/23 @ 2155 (d=1.74m)

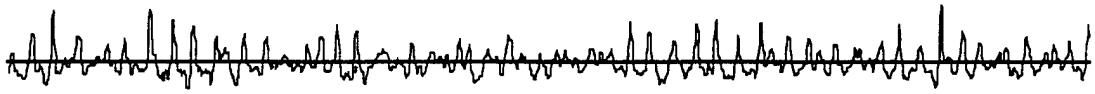

Figure 3-3 Gage 635 - 10/23 @ 2155 (d=2.83m)

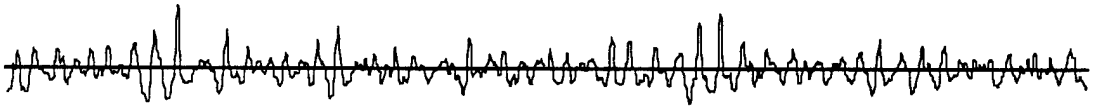

Figure 3-4 Gage 645 - 10/23 @ 2155 (d=4.31m)

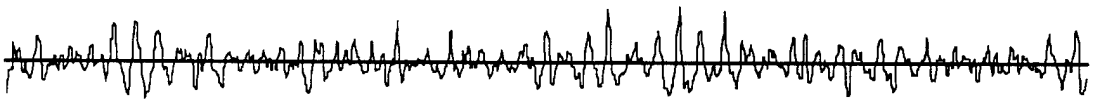

Figure 3-5 Gage 655 - 10/23 @ 2155 (d=6.0m)

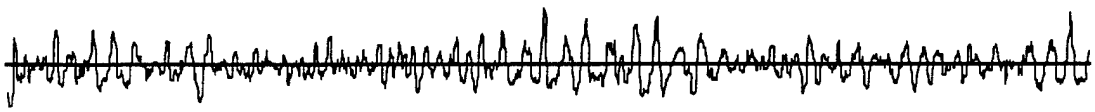

Figure 3-6 Gage 665 - 10/23 @ 2155 (d=6.08m)

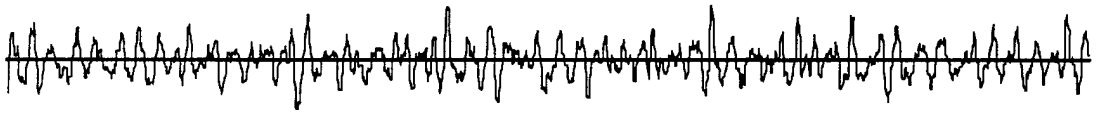

Figure 3-7 Gage 675 - 10/23 @ 2155 (d=6.82m)

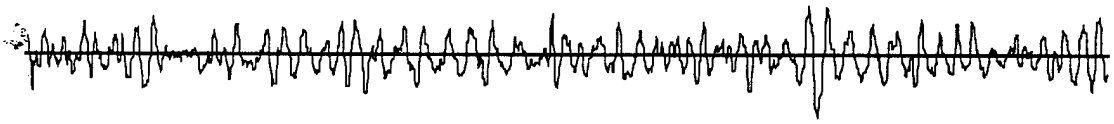

Figure 3-8 Gage 625 - 10/23 @ 2155 (d=9.66m)

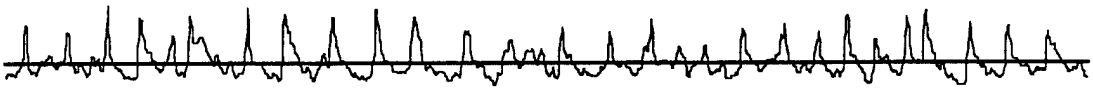

Figure 3-9 Gage 615 - 10/25 @ 1315 (d=2.23m)

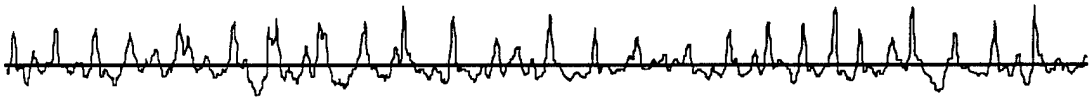

Figure 3-10 Gage 635 - 10/25 @ 1315 (d=3.32m)

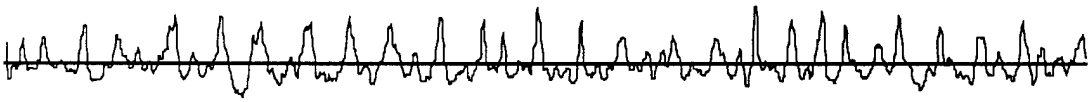

Figure 3-11 Gage 645 - 10/25 @ 1315 (d=4.66m)

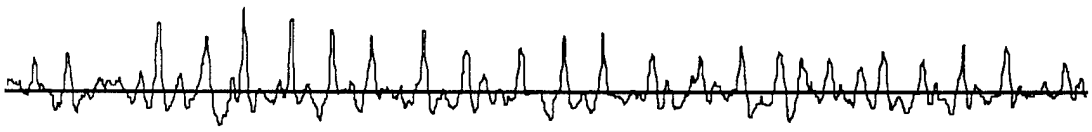

Figure 3-12 Gage 655 - 10/25 @ 1315 (d=6.44m)

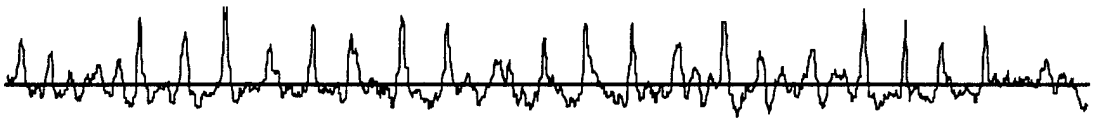

Figure 3-13 Gage 665 - 10/25 @ 1315 (d=6.52m)

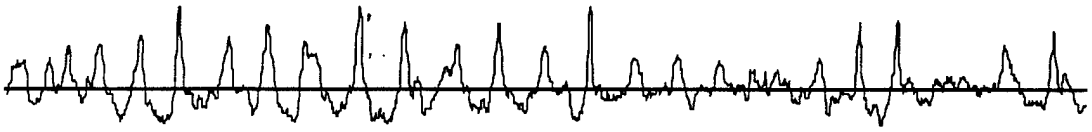

Figure 3-14 Gage 675 - 10/25 @ 1315 (d=7.22m)

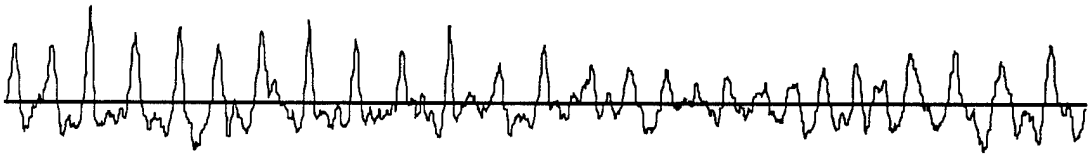

Figure 3-15 Gage 625 - 10/25 @ 1315 (d=10.04m)

3.2 Nearshore Zone Characteristics

All wave fields propagating in finite water depths are influenced by the attributes of the local sea environment. These attributes include water depth and beach slope. An awareness of the characteristics of these attributes is important to understand the type of influence they have on the wave field.

3.2.1 Discussion of Water Depth Regions During ARSLOE

Based on linear theory, there are three water depth regions which are defined using the velocity potential for a progressive wave. The velocity potential is defined as

$$\phi(x,z,t) = \frac{HgT\cosh(k(d+z))}{4\pi\cosh(kd)}\sin(kx - \frac{2\pi * t}{T}).$$

The distinct water depth regions are determined by the asymptotes of the hyperbolic function. Deep water wave data obtained at gage location 710 and shown in Table 3.1 allow these regions to be defined for the mild sea condition and the severe sea condition. In general, the deep water wave condition is defined as $kd > \pi$, where k is the wave number and h is the water depth. This condition occurs at d = 21m for the mild sea condition on 10/23 @ 2155 and d = 43m for the severe sea condition on 10/25 @ 1315. The shallow water condition is defined as $kd < \pi/10$. This condition occurs at d = 0.6m for the mild sea condition and d = 1.3m for the severe sea condition on 25 October. The intermediate water condition occurs between these bounds. All wave profile data obtained from ARSLOE are located in the intermediate water depth region.

Table 3.1 Deep Water Wave Statistics for Mild and Severe Sea Conditions

Date/Time	Zero Crossing Period, T	Deep Water Wavelength, λ_0
10/23 @ 2155	5.17 sec.	41.715 m
10/25 @ 1315	7.43 sec.	86.157 m

3.2.2 Discussion of the Surf Zone During ARSLOE

An integral aspect of any study which covers the nearshore region must analyze and consider the surf zone. The surf zone is a transient entity which varies in width offshore depending on the local sea conditions. These local conditions include the beach profile, sea severity and direction of wave field. In order to define the surf zone in this study, wave field data were analyzed which represented the range of sea conditions experienced over the two day period. The first condition, representing the mildest sea condition, was taken as 2155, 23 October 1980. The second condition, representing the most severe sea condition was taken as 1315, 25 October 1980.

Linear wave theory will be used to determine the effects of shoaling as the wave field enters shallow water. Refraction will not be considered since this process tends to reduce the shoaling wave heights and thus move the surf zone shoreward. This is shown by the definition of the refraction coefficient, $K_r = \sqrt{\frac{\cos\theta_0}{\cos\theta}}$ where θ_0 and θ are the deep water wave angle and the finite water depth wave angle respectively. This ratio will always be less than one causing a reduction in the resulting wave height. In order to ensure that conservative results are obtained, refraction will be neglected in this study. The beach profile at the ARSLOE project site shows slightly varying beach slopes so a wave breaking criteria which considers the beach slope will be used. Weggel (1972) reinterpreted laboratory results and showed a dependency of breaker height on beach slope. The following equations were used to define the surf zone locations:

Conservation of Energy: $H_2 = H_1 \sqrt{\frac{C_{g1}}{C_{g2}}}$

Breaker Criterion: $H_b = \kappa d_b$, where κ is defined by Weggel as follows:

$$\kappa = b(m) - a(m)\frac{H_b}{gT^2} \text{ with } \quad a(m) = 43.8(1.0 - e^{-19m})$$

$$b(m) = 1.56(1.0 + e^{-19.5m})^{-1}$$

As the beach slope, m approaches zero, this equation reduces to $\kappa = 0.78$. The Group Velocity, $C_g = \left(\frac{L}{T}\right)\frac{1}{2}\left(1 + \frac{2kd}{\sinh(2kd)}\right)$ will be determined based on the dispersion relation, $\left(\frac{2\pi}{T}\right)^2 = gk\tanh(kd)$, where L = wave length, T = wave period (assumed constant), g = gravitational acceleration, k = the wave number and d = local water depth.

In order to standardize the location of the surf zone, the root-mean-square wave height, H_{rms}, will be used to represent the irregular wave field. $H_{rms} = \sqrt{\frac{1}{N}\sum_{i=1}^{N} H_i^2}$ where H_i is defined as the wave height of the i^{th} wave of the irregular wave field. The surf zone which results from the use of H_{rms} will represent the approximate "center of mass" location where the most significant set of individual waves in the wave field begin to break. The surf zone calculations were based on a root-mean-square wave height that was determined from the deep water wave displacement data. This single wave height was used to represent the irregular sea and shoaled landward. Since the real sea will have a significant number of waves with heights larger and smaller than the root-mean-square, the actual breaking zone is an obscure entity. This technique for determining the surf zone locations is adequate to make general comparisons when analyzing the spatial changes in the nonlinearity of the irregular sea in finite water depths. The surf zone locations during the mildest and most severe sea conditions over the two day period are shown in Table 3.2.

In Table 3.2 it is shown that during the mild sea condition, the breakpoint, indicating the beginning of the surf zone, is located 70 meters from the shoreline in 1.51 meters of water. This breakpoint is the location where a wave having a height equivalent to the

root-mean-square wave height of the wave field will break. During the severe sea condition, this breakpoint occurs 110 meters from the shoreline in 3.32 meters of water. Realistically, waves would be observed breaking considerably seaward of the breakpoints determined in the respective sea conditions due to the spectrum of wave heights present in an irregular sea. The root-mean-square wave height breakpoint is used in order to standardize the position of the surf zone for camparison purposes.

Table 3.2 Surf Zone Locations for Mild and Severe Sea Conditions

Sea Condition	Depth where a wave with height H_{rms}, Breaks	Start of Surf Zone -Dist. from Shore-
Mild - 10/23 @ 2155	1.51 m	70 m
Severe - 10/25 @ 1315	3.32 m	110 m

3.3 Non-Gaussian Probability Density Function

The probabilistic approach used in this study will make use of the probability density function applicable to non-gaussian random processes developed by Ochi and Ahn (1994a). This probability density function appears to represent non-Gaussian waves in shallow and intermediate water depths as well as Gaussian waves in deep water.

3.3.1 Non-Gaussian Probability Density Function Background

The probability density function has a background of the Kac-Siegert solution developed for the response of non-linear systems. The density function, y(t), is given as the sum of the standardized normal variates and its squares as follows

$$y(t) = \sum_{j=1}^{N} (\beta_j Z_j + \lambda_j Z_j^2)$$

The parameters β_j and λ_j are determined by finding the eigenfunction and eigenvalues of the integral equation given by

$$\int K(\omega_1,\omega_2)\psi_j(\omega_2)d\omega_2 = \lambda_j\psi_j(\omega_1)$$

where $K(\omega_1, \omega_2) = H(\omega_1, \omega_2)\sqrt{S(\omega_1)S(\omega_2)}$

$\psi_j(\omega)$ = orthogonal eigenfunction = $\begin{cases} \int \psi_j(\omega)\psi_k(k)d\omega = 1 \text{ for } j = k \\ \text{otherwise, } \psi_j(\omega) = 0 \end{cases}$

$H(\omega_1, \omega_2)$ = second order frequency response function

$S(\omega)$ = output spectral density function

As can be seen from the form of this solution, the probability density function of y(t), can not be found without knowledge of the second order frequency response function, $H(\omega_1, \omega_2)$ and there is no way to evaluate this response function for irregular seas. Ochi and Ahn showed however, that Kac-Siegerts' solution can be obtained from the time history of the wave record without any knowledge of the second order frequency response function, $H(\omega_1, \omega_2)$. The probability density function thus obtained for describing non-gaussian random processes is

$$f(x) = \frac{1}{\sqrt{2\pi}\sigma_*}\exp\left[-\frac{1}{2(\gamma a\sigma_*)^2}(1-\gamma a\mu_* - \exp(-\gamma a x))^2 - \gamma a x\right]$$

where, $\gamma = \begin{cases} 1.28 \, for: x \geq 0 \\ 3.00 \, for: x < 0 \end{cases}$.

The parameters, a, μ_* and σ^2_* are determined from the cumulants evaluated from the wave data. These cumulants are related to the β_j and λ_j values of the Kac-Siegert solution by the following relationships

$$k_1 = \sum_{j=1}^{2N} \lambda_j$$

$$k_2 = \sum_{j=1}^{2N} \beta^2{}_j + \sum_{j=1}^{2N} \lambda^2{}_j$$

$$k_3 = 6\sum_{j=1}^{2N} \beta^2{}_j\lambda_j + 8\sum_{j=1}^{2N} \lambda^3{}_j \text{ , etc.}$$

In the present study, k_1 represents the mean water level and is therefore defined by, $k_1 = 0$. k_2 and k_3 are equal to the data sample moments, $E[x^2]$ and $E[x^3]$ respectively. Based on this relationship, the parameters, a, μ_* and σ^2_* can be determined through the iterative solution of three equations along with the analysis of a data record for the non-Gaussian random process being analyzed. The three equations are

$$a\,\sigma^2_* + a\,\mu_*^2 + \mu_* = E[x] = 0$$

$$\sigma^2_* - 2a^2\sigma^4_* = E[x^2]$$

$$2a\,\sigma^4_*(3 - 8a^2\sigma^2_*) = E[x^3]$$

3.3.2 Probability Density Function Application to Wave Data

In order to determine values for the three parameters, a, μ_* and σ^2_*, which are used to define the degree of non-linearity a shoaling wave field has at a given location and sea state, data records must be analyzed. With the applicability of the probability density function verified based on the wave data collected during ARSLOE, the approximately 1000 data records from 1200 on 23 October to 1315 on 25 October will be analyzed to determine values for the three parameters defining the probability density function. The procedure used during this study to perform this task is as follows:

- Compute the standard deviation of each twenty minute wave record consisting of 4800 discrete wave displacement data points $E(x^2) = \frac{1}{n}\sum_i x^2{}_i$.

(E[x] does not need to be computed since it is defined as zero and the data are already standardized).

- Compute the third moment of the same twenty minute wave record $E(x^3) = \frac{1}{n}\sum_i x^3{}_i$.

- Define the standard deviation of the data record as $\sigma = \sqrt{E(x^2)}$.

- Evaluate the three parameters, a, μ_* and σ^2_*, through iterative solution of the following three equations:

$$a\,\sigma^2_* + a\,\mu_*^2 + \mu_* = E[x] = 0$$

$$\sigma^2_* - 2a^2\sigma^4_* = E[x^2]$$

$$2a\,\sigma^4_*(3 - 8a^2\sigma^2_*) = E[x^3].$$

It is important to note that the standard deviation of the data record is used in the analysis as an indicator of the sea severity and not the significant wave height. This is because the definition of significant wave height is not applicable to non-Gaussian waves.

All available data sets covering the seven finite water depth gage locations between 1200, 23 October 1980 and 1400, 25 October 1980 were analyzed and a, μ_* and σ^2_* were determined.

Based on a plot of the individual parameters in the space domain, it was determined that a smoothing technique should be used to refine the "a" parameter values. This smoothing was done in order to remove the sporadic tertiary effects while ensuring the smoothed "a" value does not lose any authenticity. An exponential smoothing technique was used which resulted in the lowest mean absolute deviation (MAD) between the raw "a" parameter value and the smoothed "a" parameter. The remaining two parameters, μ_* and σ^2_* did not show the same susceptibility to tertiary effects so no smoothing was done. Comparisons between the actual and smoothed "a" parameters are shown in Appendix A for all Gage positions.

3.3.3 Dimensional Analysis of PDF Parameters

For each of the approximately one-hundred-fifty data sets per gage position, the probability density function parameters, a, μ_* , σ_* were determined iteratively. Each of the parameters contain discrete dimensions. Based on dimensional analysis, these

dimensions are as follows: It is known that k_2, representing the data sets' variance has dimensions of $[L^2]$. It is also known that k_3, representing the data sets' third moment has dimensions of $[L^3]$. It follows from the knowledge of these dimensions that the parameters, a, μ_* , σ_* must have dimensions [1/L], [L] and [L] respectively.

In order to minimize any dependence on external conditions and to ensure the solutions are universally applicable, these parameters, a, μ_* , σ_* must be made non-dimensional. The non-dimensional quantities that will be used in this study are, $a\sigma$, μ_*/σ, σ_*/σ and σ/d. σ is defined as the standard deviation of that wave displacement data and d is defined as the water depth.

CHAPTER 4
PROBABILITY DENSITY FUNCTION ANALYSIS

4.1 Probability Density Function Applicability Verification

As stated in the introduction, one of the objectives of this study is to determine whether or not the probability density function developed by Ochi and Ahn is valid for representing waves in finite water depths. To verify the applicability of this probability density function, wave displacement data sets obtained from the ARSLOE experiment were used in comparing the histogram of the data record to the probability density function. Each data set contained 4800 wave displacement readings taken over a twenty minute period. To ensure a thorough verification of the probability density function, the data records used for the analysis were from all seven "finite" water depth gage locations and analysis was done over a wide range of sea state conditions. One analysis was done on data from 23 October 1980 at 2155. This represented a mild sea state. The other analysis was done on data from 25 October 1980 at 1315. This data set was at the peak of the most severe storm experienced during the entire ARSLOE study.

Figures 4.1-4.14 show comparisons between the histogram data and the non-Gaussian probability density function. Included also in the figures is the Gaussian (normal) probability density function for comparison. Figures 4.1-4.7 pertain to the mild sea condition while Figures 4.8-4.14 represent the severe sea condition. As can be seen from these figures, the probability density function agrees very well with the histogram generated from the data record in all cases. This implies that the probability density function derived by Ochi and Ahn can be used with confidence when analyzing non-Gaussian random processes such as wave displacements in shallow and intermediate

waters. It can also be seen that the probability density function approximates the normal distribution when the wave field is in the deeper intermediate water condition under mild sea conditions.

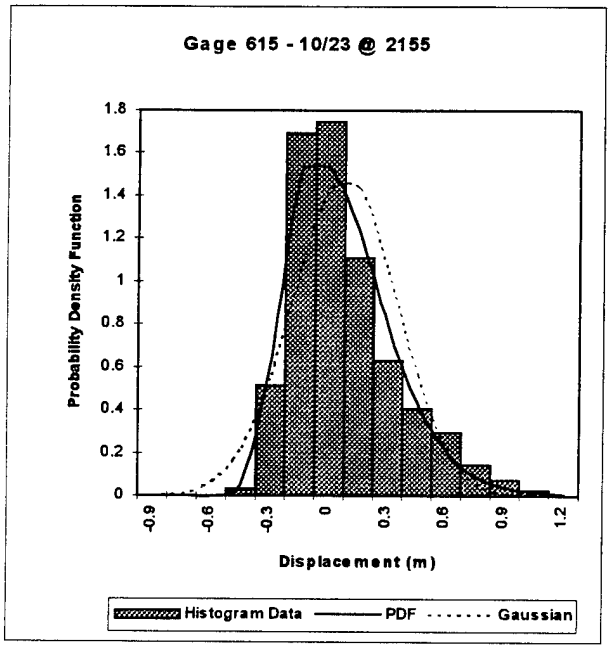

Figure 4.1 Histogram Data

Table 4.1 Gage 615 - 10/23 @ 2155

	WAVE PROPERTIES
615	10/23 @ 2155
a (1/m)	.572645
μ_* (m)	-.04948
σ_* (m)	.275683
σ (m)	.267219
d (m)	1.74
σ/d	.153574

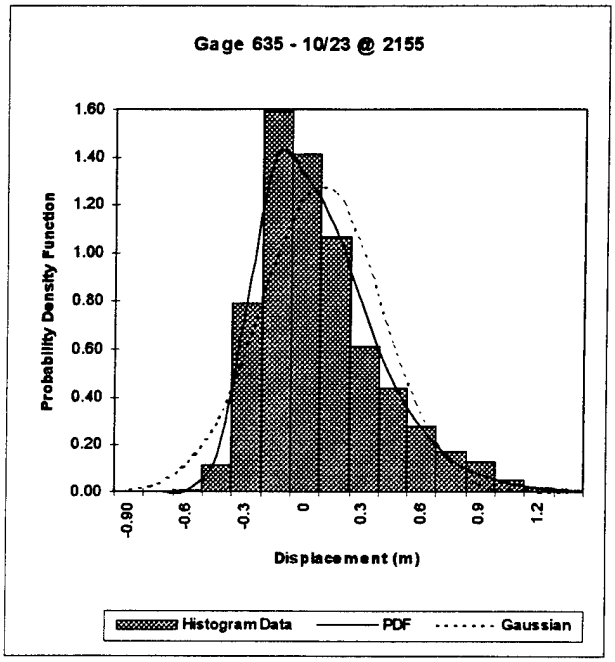

Figure 4.2 Histogram Data

Table 4.2 Gage 635 - 10/23 @ 2155

	WAVE PROPERTIES
635	10/23 @ 2155
a (1/m)	.481441
μ_* (m)	-.0547
σ_* (m)	.318871
σ (m)	.30989
d (m)	2.83
σ/d	.109502

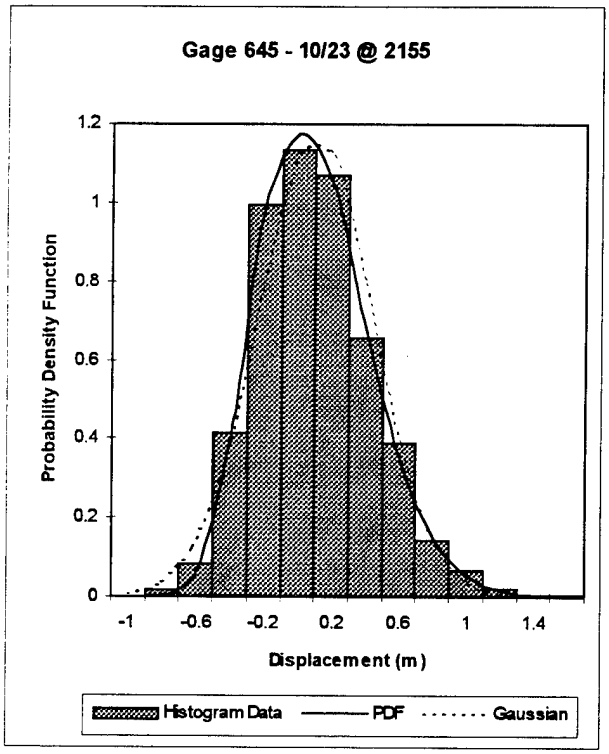

Figure 4.3 Histogram Data

Table 4.3 Gage 645 - 10/23 @ 2155

	WAVE PROPERTIES
645	10/23 @ 2155
a (1/m)	.200988
μ_* (m)	-.03084
σ_* (m)	.343446
σ (m)	.340708
d (m)	4.31
σ/d	.079051

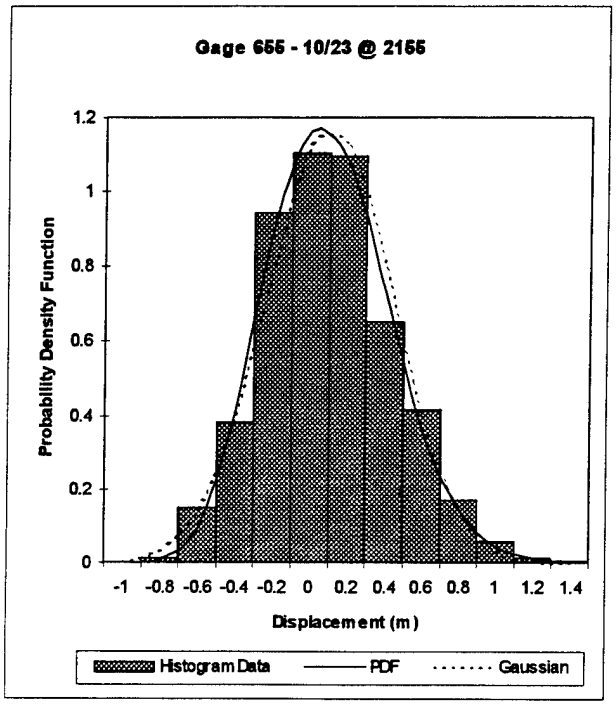

Figure 4.4 Histogram Data

Table 4.4 Gage 655 - 10/23 @ 2155

	WAVE PROPERTIES
655	10/23 @ 2155
a (1/m)	.104437
μ_* (m)	-.01771
σ_* (m)	.340056
σ (m)	.339137
d (m)	6.0
σ/d	.056523

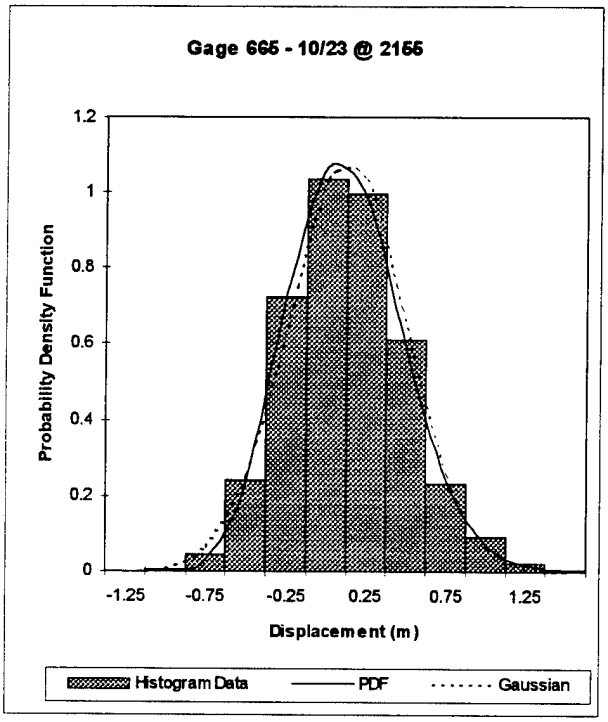

Figure 4.5 Histogram Data

Table 4.5 Gage 665 - 10/23 @ 2155

	WAVE PROPERTIES
665	10/23 @ 2155
a (1/m)	.126266
μ_* (m)	-.01835
σ_* (m)	.365155
σ (m)	.364236
d (m)	6.08
σ/d	.059907

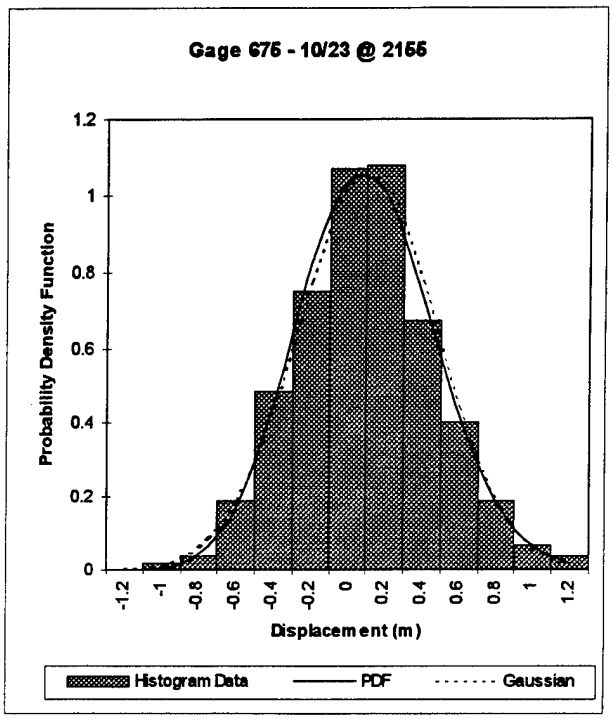

Figure 4.6 Histogram Data

Table 4.6 Gage 675 - 10/23 @ 2155

	WAVE PROPERTIES
675	10/23 @ 2155
a (1/m)	.094349
μ_* (m)	-.01014
σ_* (m)	.375221
σ (m)	.374948
d (m)	6.82
σ/d	.054978

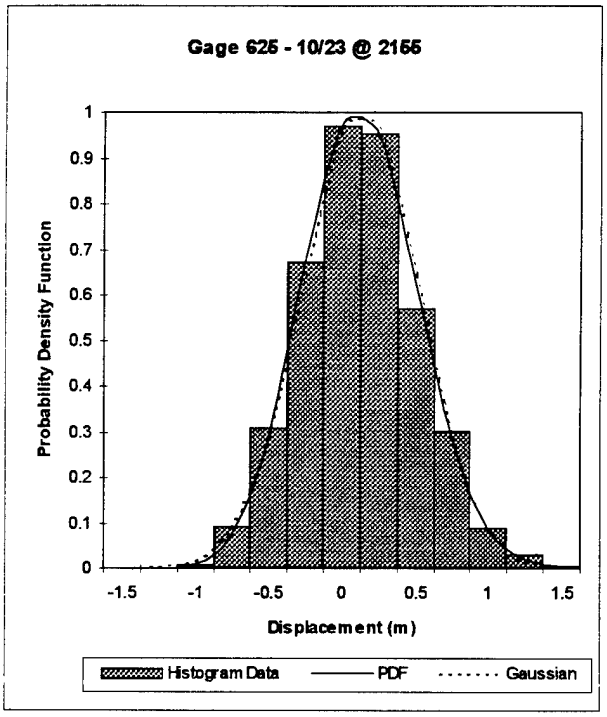

Figure 4.7 Histogram Data

Table 4.7 Gage 625 - 10/23 @ 2155

	WAVE PROPERTIES
625	10/23 @ 2155
a (1/m)	.069914
μ_* (m)	-.00819
σ_* (m)	.394571
σ (m)	.394401
d (m)	9.66
σ/d	.040828

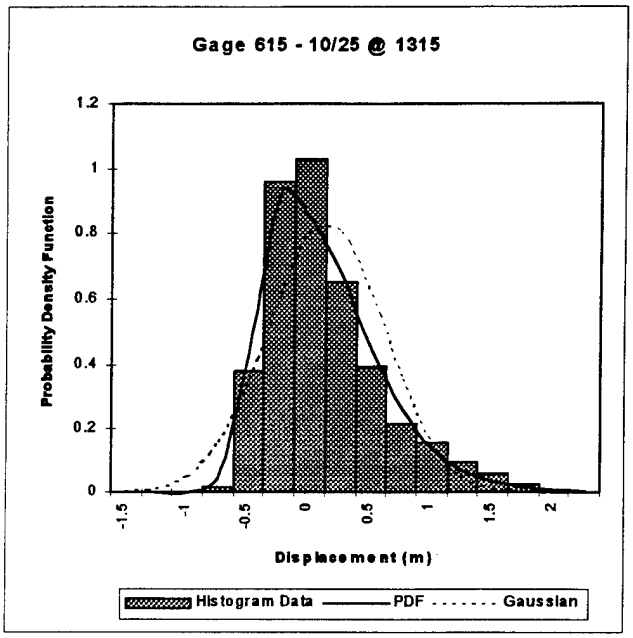

Figure 4.8 Histogram Data

Table 4.8 Gage 615 - 10/25 @ 1315

	WAVE PROPERTIES
615	10/25 @ 1315
a (1/m)	.372027
μ_* (m)	-.09863
σ_* (m)	.498230
σ (m)	.47981
d (m)	2.23
σ/d	.215161

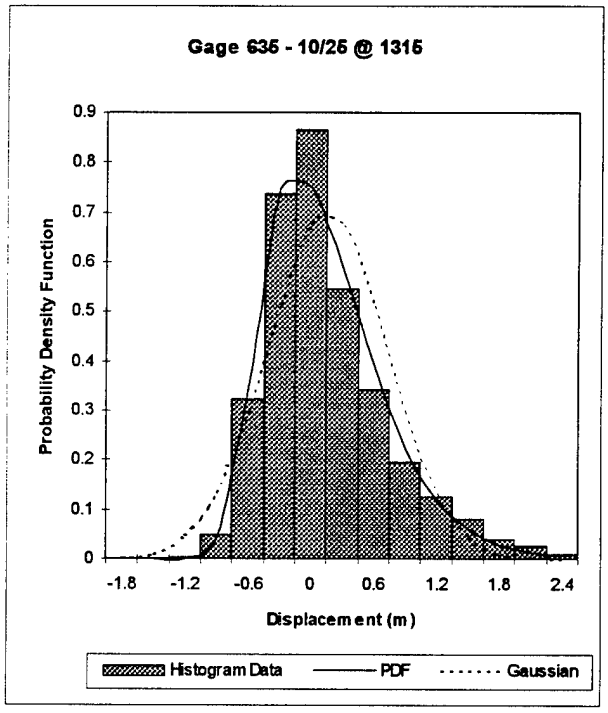

Figure 4.9 Histogram Data

Table 4.9 Gage 635 - 10/25 @ 1315

	WAVE PROPERTIES
635	10/25 @ 1315
a (1/m)	.318011
μ_* (m)	-.10497
σ_* (m)	.591069
σ (m)	.573397
d (m)	3.32
σ/d	.17271

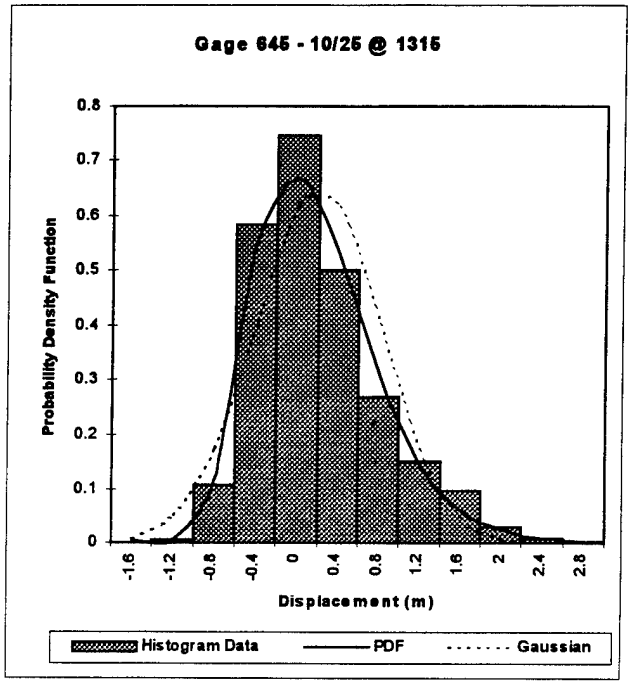

Figure 4.10 Histogram Data

Table 4.10 Gage 645-10/25 @ 1315

	WAVE PROPERTIES
645	10/25 @ 1315
a (1/m)	.256391
μ_* (m)	-.10245
σ_* (m)	.628243
σ (m)	.612186
d (m)	4.66
σ/d	.13137

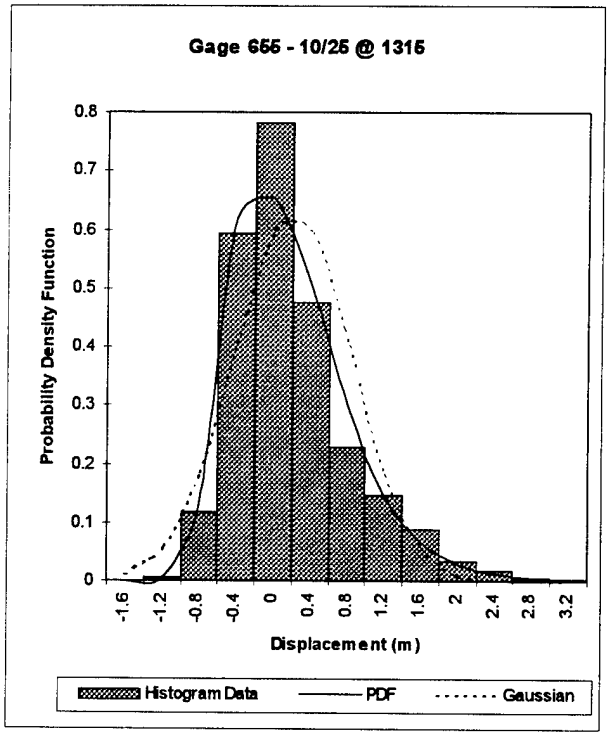

Figure 4.11 Histogram Data

Table 4.11 Gage 655 -10/25 @ 1315

	WAVE PROPERTIES
655	10/25 @ 1315
a (1/m)	.269927
μ_* (m)	-.12356
σ_* (m)	.658813
σ (m)	.636821
d (m)	6.44
σ/d	.098885

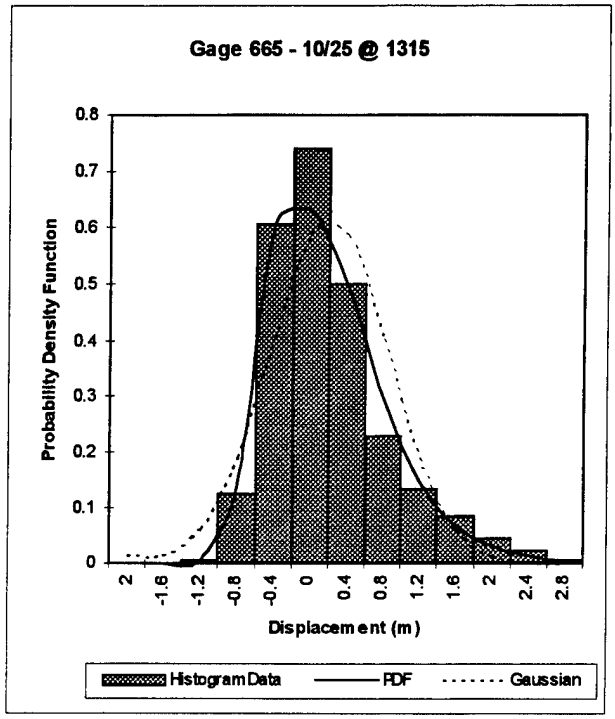

Figure 4.12 Histogram Data

Table 4.12 Gage 665 -10/25 @ 1315

	WAVE PROPERTIES
665	10/25 @ 1315
a (1/m)	.269743
μ_* (m)	-.12978
σ_* (m)	.67434
σ (m)	.650698
d (m)	6.52
σ/d	.09980

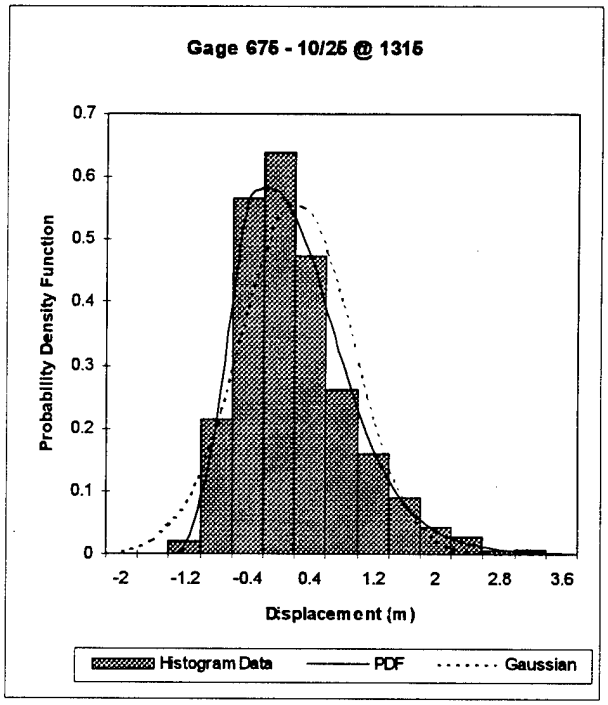

Figure 4.13 Histogram Data

Table 4.13 Gage 675 -10/25 @ 1315

	WAVE PROPERTIES
675	10/25 @ 1315
a (1/m)	.220143
μ_* (m)	-.12062
σ_* (m)	.727669
σ (m)	.708477
d (m)	7.22
σ/d	.098127

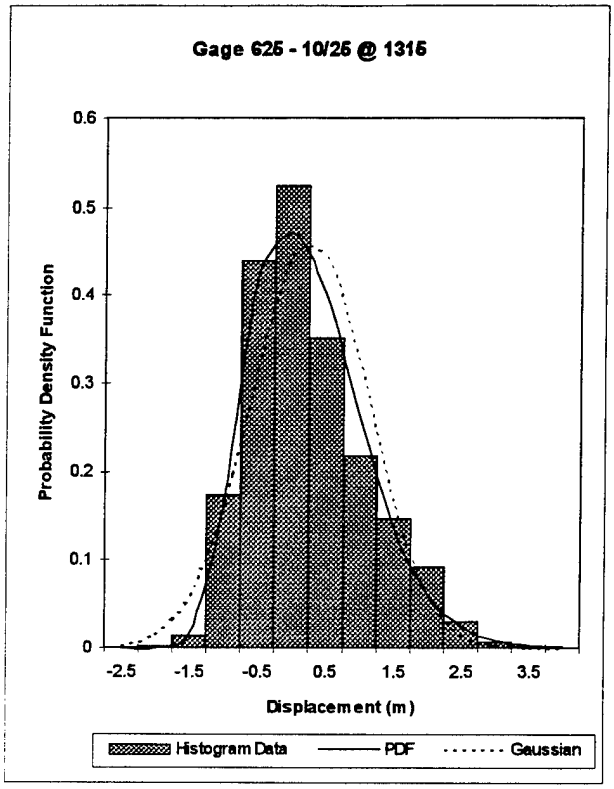

Figure 4.14 Histogram Data

Table 4.14 Gage 625 -10/25 @ 1315

	WAVE PROPERTIES
625	10/25 @ 1315
a (1/m)	.140009
μ_* (m)	-.10961
σ_* (m)	.872244
σ (m)	.858792
d (m)	10.04
σ/d	.085537

Based on a comparison with the water depth regions defined in Section 3.2.1, it can be seen that the histogram data and the probability density function closely resemble the normal distribution even after the wave field enters intermediate water for milder sea conditions. This is shown in Figures 4.6 and 4.7. This implies that the characteristics of the wave profile are dependent on the sea condition as well as the water depth.

The histogram data for both the mild and severe sea conditions in Figures 4.1-4.14 show the distribution of the wave profiles progressively becomes more non-Gaussian as the waves propagate toward shallower depths. The non-Gaussian trend becomes more extreme as the sea condition becomes more severe. It is significant to note also that the

non-Gaussian characteristics are most pronounced at the shallower gage locations, Gages 615 and 635.

4.2 Gaussian/non-Gaussian Boundary Definition

The histogram data shown in Figures 4.1 - 4.14 represent the same wave profiles depicted in Figures 3.2 - 3.15. The transformation from Gaussian to non-Gaussian profiles begin with subtle changes in the amplitude of the negative displacements and the width of the troughs. This initial transformation can be seen be comparing Figures 4.4 and 4.6. Figure 4.6 shows a nearly normal distribution. Figure 4.4 shows a slight elevation of the apex and a narrowing of the negative tail. It is also significant to note that the positive part of the distribution remains relatively unchanged. This indicates that the initial changes affect the trough region of the profile more drastically than the positive region. Figure 4.4 demonstrates that the trough region becomes shallower and wider. As the profile continues to shoal, changes begin to occur in the positive displacement region of the distribution. The peaks become narrower and higher. This can be seen graphically by comparing Figures 4.2 and 4.4. The positive region of the wave profile is not as full when compared with the normal distribution and the positive tail extends farther than the normal curve.

As described above, significant transformations occur in the wave profile as the wave train propagates into shallower water. There is a point in this transformation when the wave profile deviates significantly enough from the normal distribution that the waves can no longer be considered a Gaussian random process. Identification of this boundary is important to ensure assumptions made regarding the waves remain valid. Analysis of the histogram data shows that the non-Gaussian characteristics of coastal waves depends on water depth and sea severity. Based initially on analysis of the histogram data shown in Figures 4.5 and 4.6, it appears this transition boundary occurs when the non-dimensional,

wave standard deviation, σ/d, is approximately 0.06. The non-dimensional parameter, σ/d, is used because it considers both sea severity and water depth. Eight random sea conditions were selected having σ/d values between 0.04 and 0.10. These eight data sets are depicted in Figure 4.15 in terms of aσ as a function of σ/d . The data points labeled A-H in Figure 4.23, each correspond to a distribution shown in Figures 4.15-4.23. Data points A-G were intentionally grouped around the 10 meter water depth. This minimized any impact water depth and/or beach slope may have on the analysis results. The statistical data for these points are provided in Table 4.15.

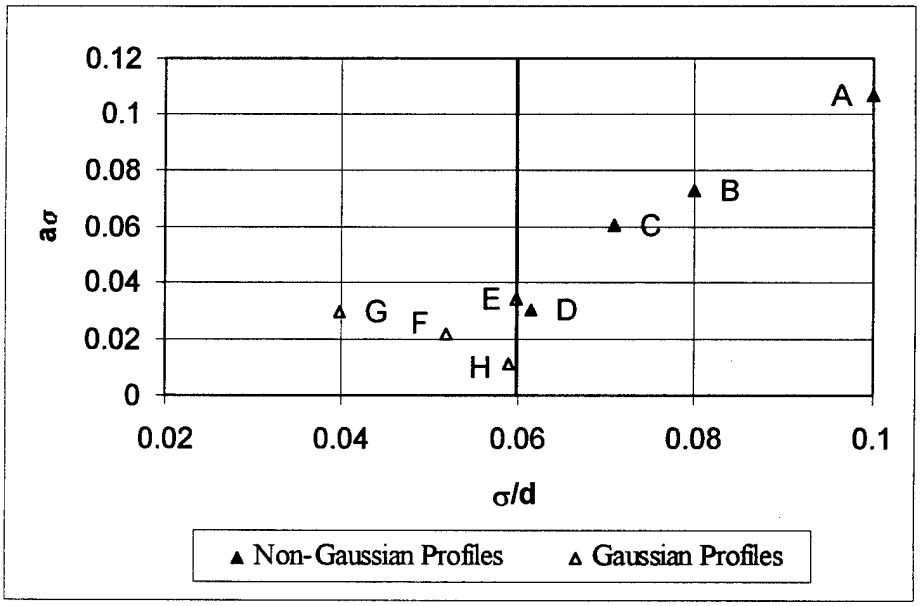

Figure 4.15 Sample Data Points to Analyze Gaussian/Non-Gaussian Boundary

Table 4.15 Statistical Properties of Data Points A-H of Figure 4.15

POINT	σ/d	H_s	Water Depth, d
A	0.1000	3.08 m	9.51 m
B	0.0800	2.74 m	9.67 m
C	0.0710	2.47 m	9.64 m
D	0.0616	2.47 m	10.03 m
E	0.0600	2.43 m	10.13 m
F	0.0520	1.78 m	8.90 m
G	0.0398	1.57 m	9.88 m
H	0.0590	4.77 m	20.20 m

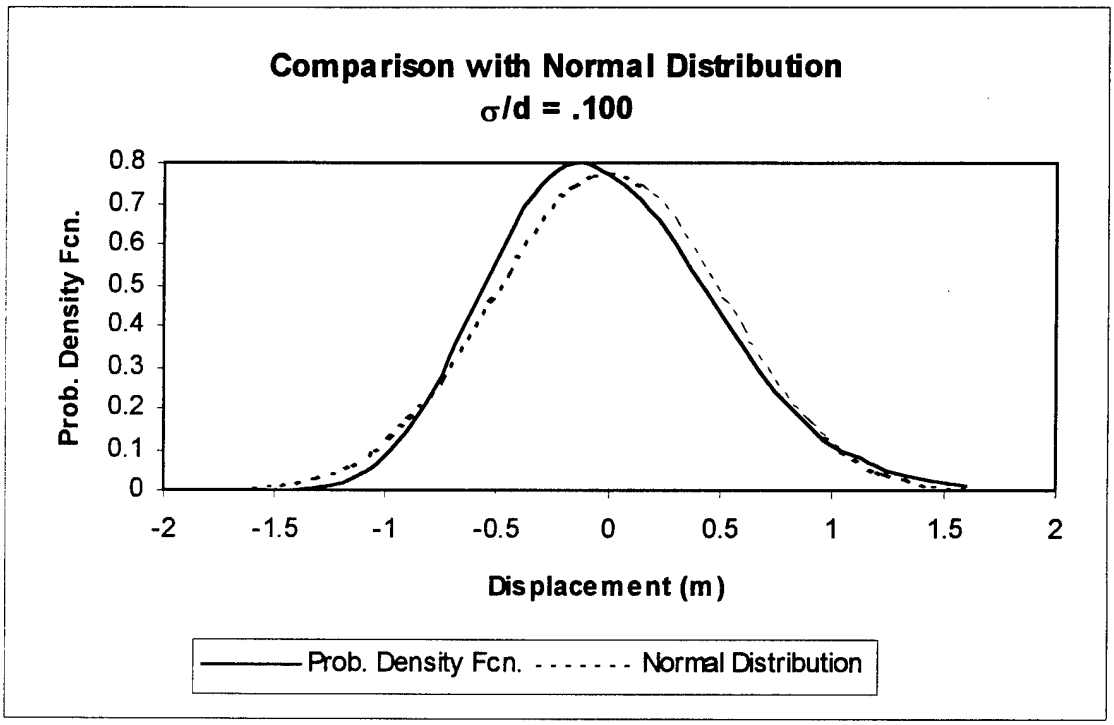

Figure 4.16 Point A of Figure 4.15

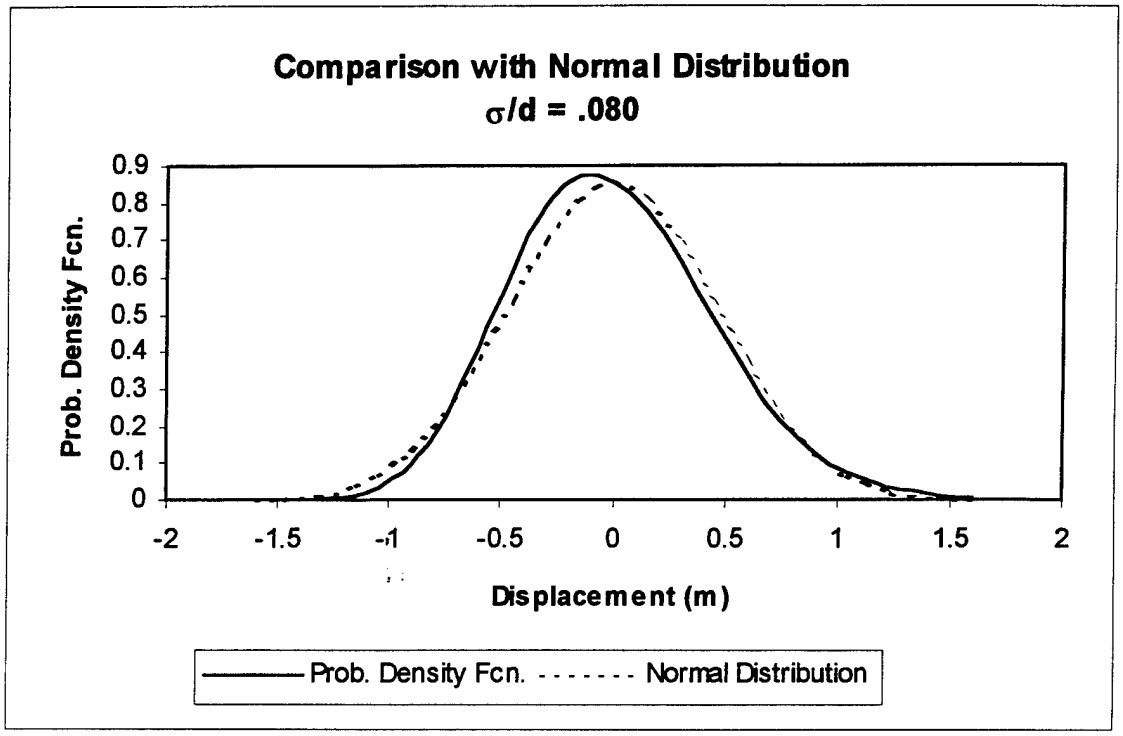

Figure 4.17 Point B of Figure 4.15

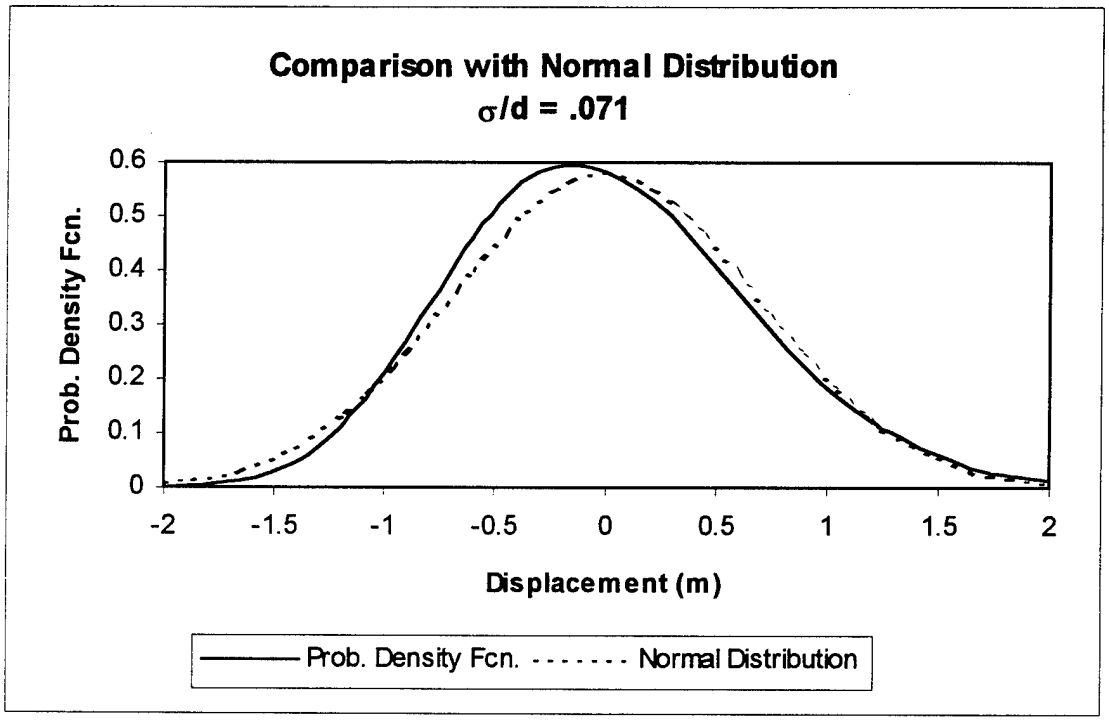

Figure 4.18 Point C of Figure 4.15

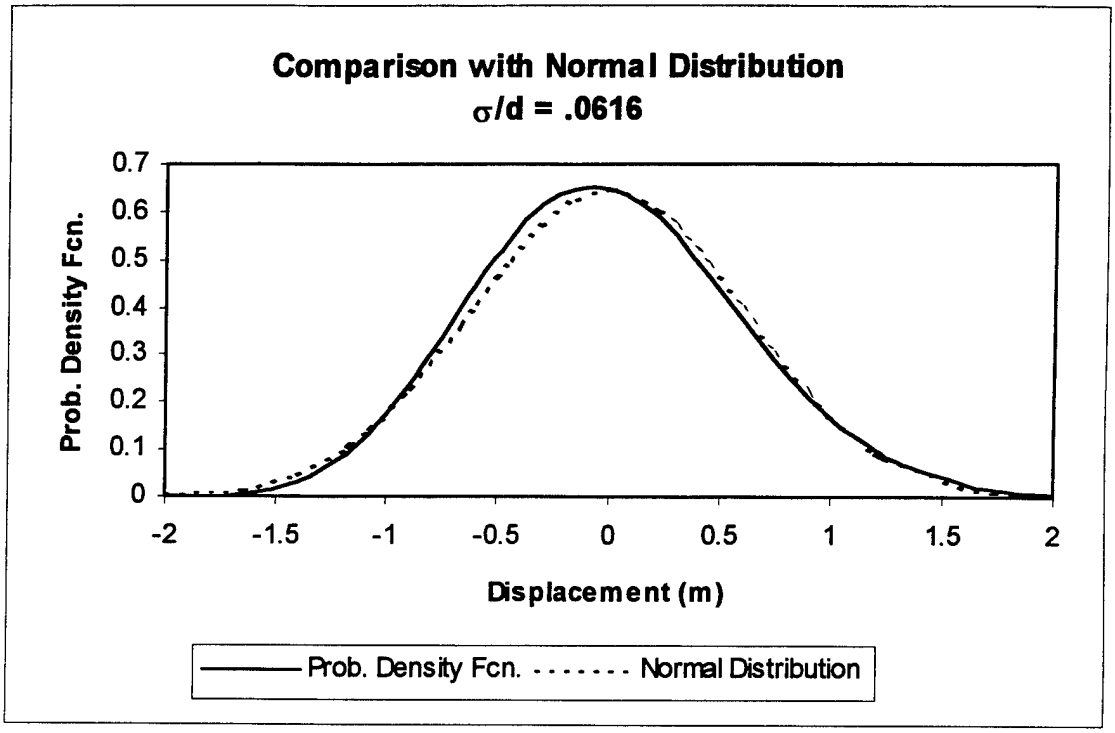

Figure 4.19 Point D of Figure 4.15

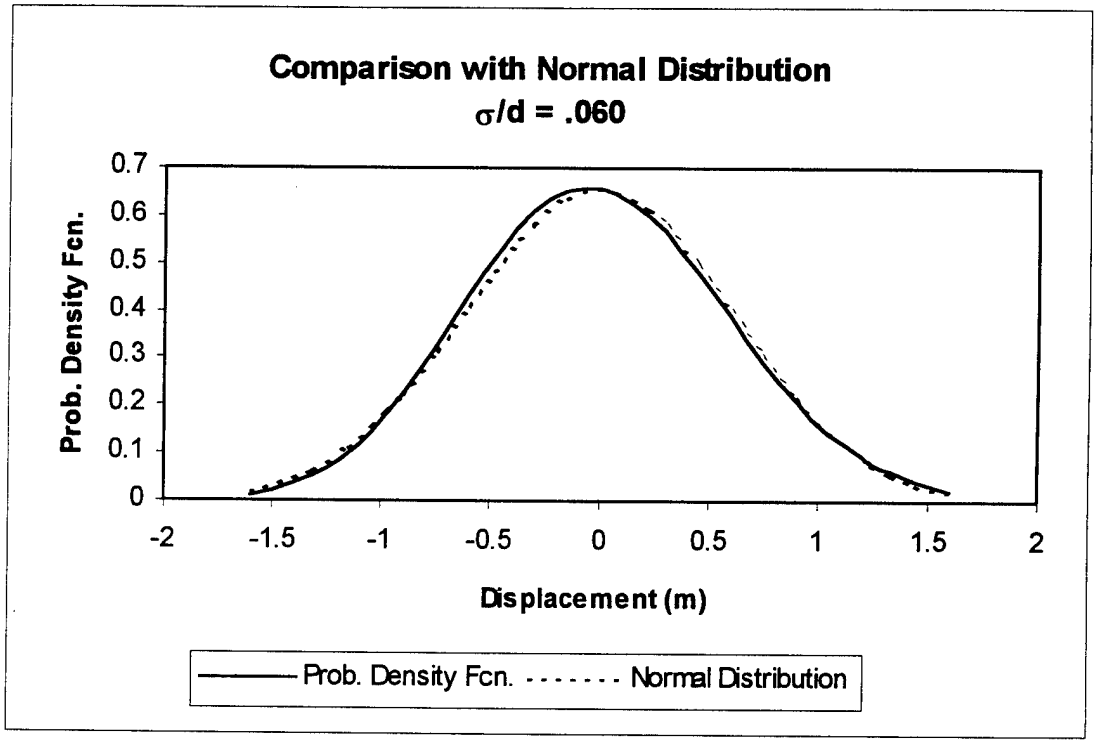

Figure 4.20 Point E of Figure 4.15

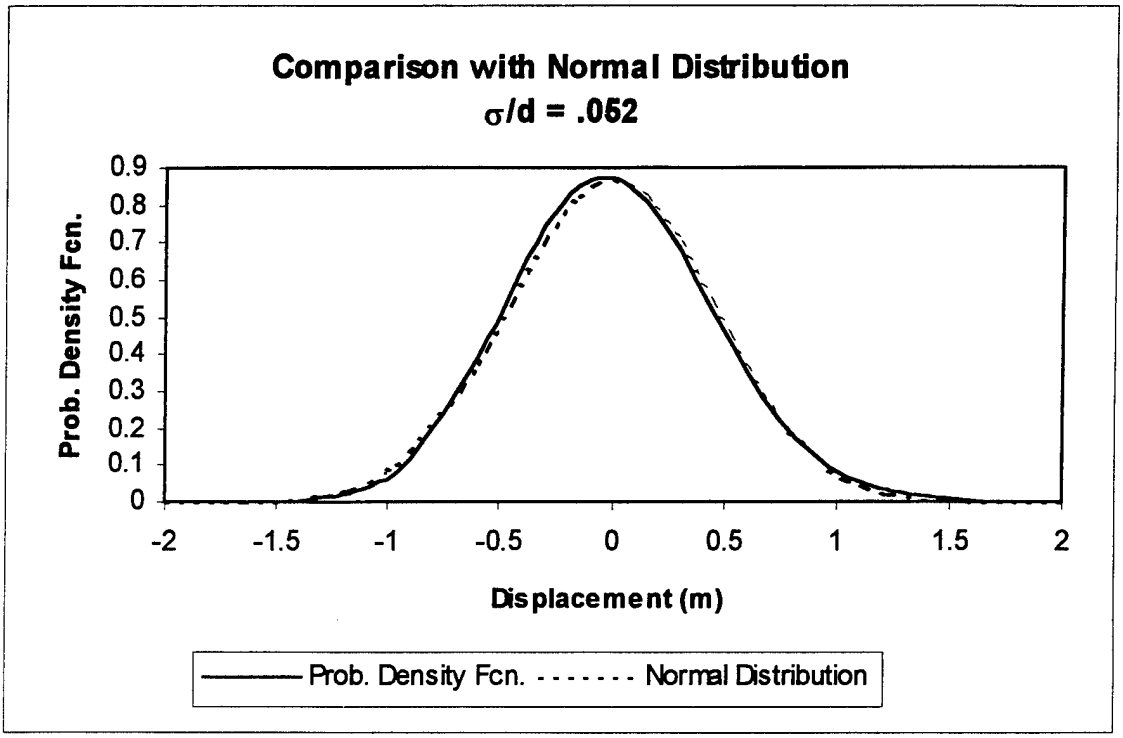

Figure 4.21 Point F of Figure 4.15

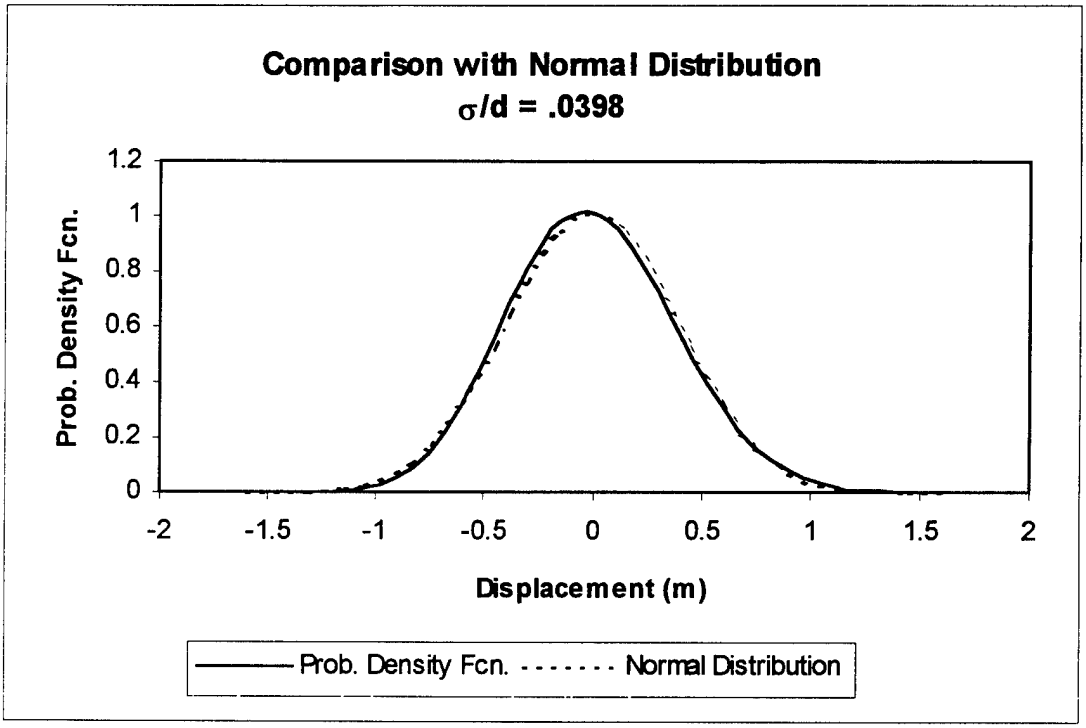

Figure 4.22 Point G of Figure 4.15

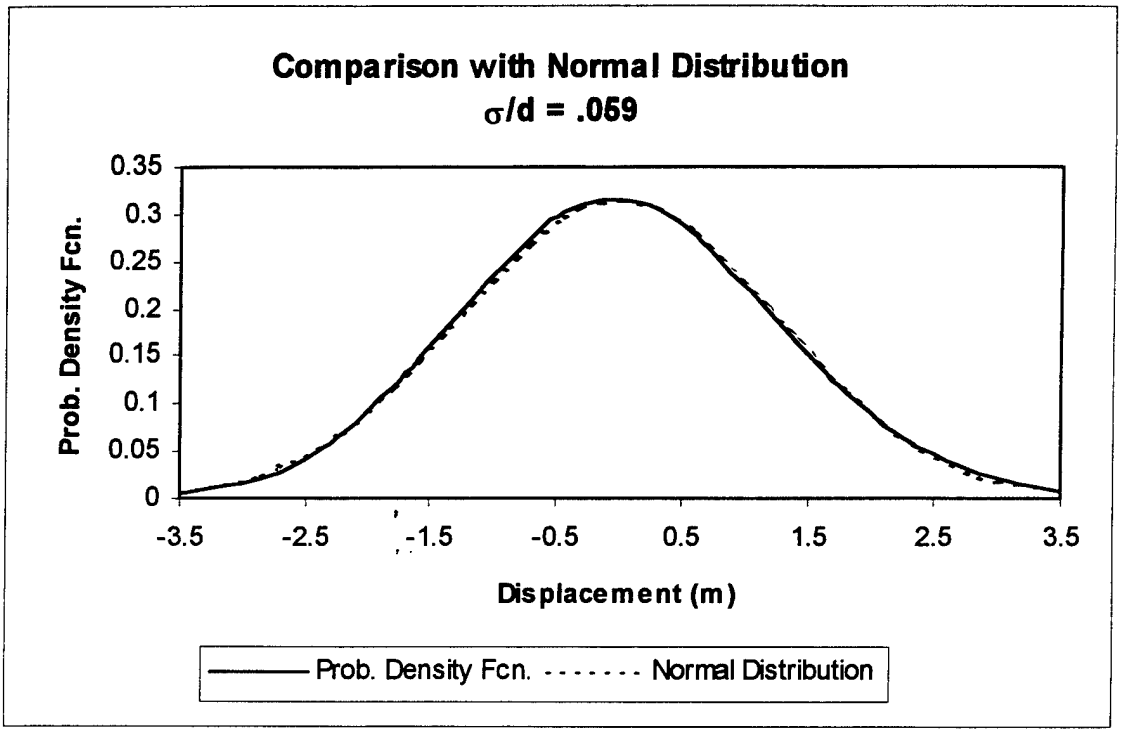

Figure 4.23 Point H of Figure 4.15

Figures 4.16 - 4.23 confirm that the region between $\sigma/d = 0.06$ and $\sigma/d = 0.08$, shown in Figures 4.20 and 4.17 respectively, appears to be when the wave profile transforms from Gaussian to non-Gaussian. A closer inspection of this region is shown in Figures 4.18 - 4.20. The distribution shows a considerable increase in deviation from the normal between $\sigma/d = 0.06$ and $\sigma/d = 0.0616$ as shown in Figures 4.20 and 4.19 respectively.

Due to the subjective nature of this boundary, a general boundary can be defined based on probabilistic analysis. This boundary, defining the conditions under which the wave profile can no longer be considered Gaussian, occurs when $\sigma/d = 0.06$.

A similar study was conducted by Ochi and Wang (1984); however, they defined the boundary condition between Gaussian and non-Gaussian wave profiles in terms of the wave record parameter, λ_3. λ_3 represents the skewness of the wave profile which they determined to be the dominant parameter affecting the non-Gaussian characteristics of

coastal waves. Ochi and Wang concluded that coastal waves in seas for which λ_3 is less than 0.2 can be considered as a Gaussian random process. For comparison purposes, this boundary condition is plotted along with the findings of this present study in Figure 4.24. In terms compatible with the approach of this present study, their boundary condition can be defined as $\sigma / d = 0.0543$. It is encouraging that there shows very close agreement between both findings. Additional analysis was contributed by Ochi and Ahn (1994b) whose data points are shown in Figure 4.24 as white circles. Ochi and Ahn (1994b) defined the transition criterion between Gaussian and non-Gaussian as occurring when $a < 0.01$ where "a" is one of the parameters in the non-Gaussian probability density function. The white circle data points define the limiting cases based on his criterion. This third method for determining the boundary between Gaussian and non-Gaussian wave profiles agrees very well with the other two further verifying the validity of this finding.

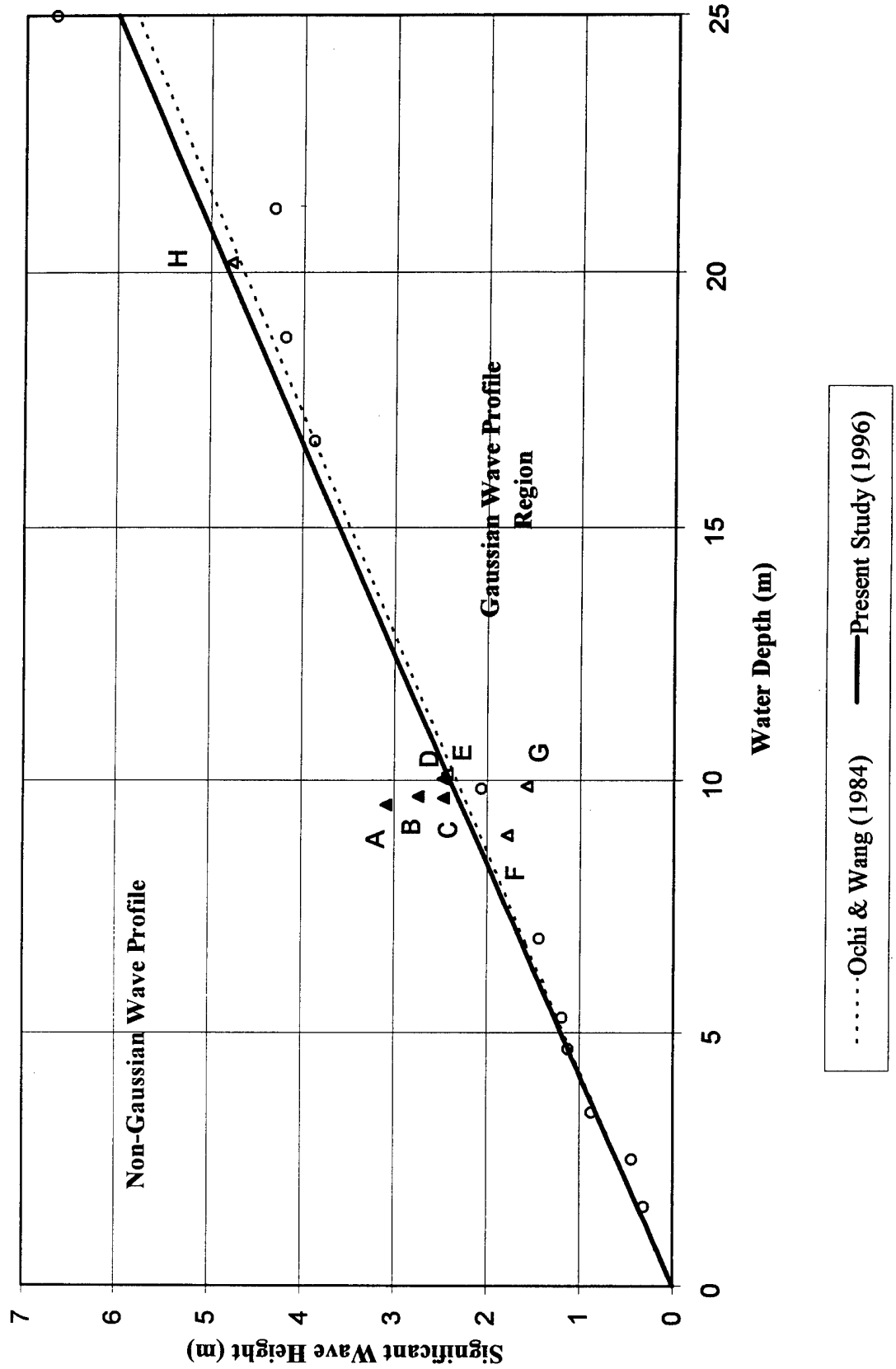

Figure 4.24 Gaussian/Non-Gaussian Boundary Defined

CHAPTER 5
TREND ANALYSIS OF PARAMETERS

5.1 Relationship between σ and Water Depth

As was discussed earlier, the distribution of the wave profile is highly dependent on sea severity and water depth with sea severity being defined in terms of the wave profiles' standard deviation, σ. Since these two terms will be used considerably in the following trend analyses, their relationship with each other will be examined.

Figure 5.1 shows examples of simultaneous measurements of σ plotted as a function of distance offshore for two cases. It is evident from Figure 5.1, that the standard deviation of the wave profile is influenced by water depth. As water depth decreases, the relative magnitude of the standard deviation decreases. It is also seen that for more severe sea conditions, represented by 10/25 @ 1315 data in Figure 5.1, the overall change in σ as the wave field propagates into shallower waters is greater as compared with milder sea conditions (10/23 @ 2155). Based on theoretical considerations of σ, it can be assumed that σ approaches zero as distance offshore approaches zero. This trend is observed in Figure 5.1 since both cases shown appear to converge to the origin. From the information on the surf zone locations for these two cases computed in Chapter 3, it appears that σ begins to decrease rapidly towards zero once the break point is reached.

The information shown in Figure 5.1 based on two cases is shown in Figure 5.2 for all data sets analyzed in this study. Instead of σ being plotted as a function of distance offshore, Figure 5.2 plots σ as a function of water depth. This will take into consideration any local changes in mean sea level.

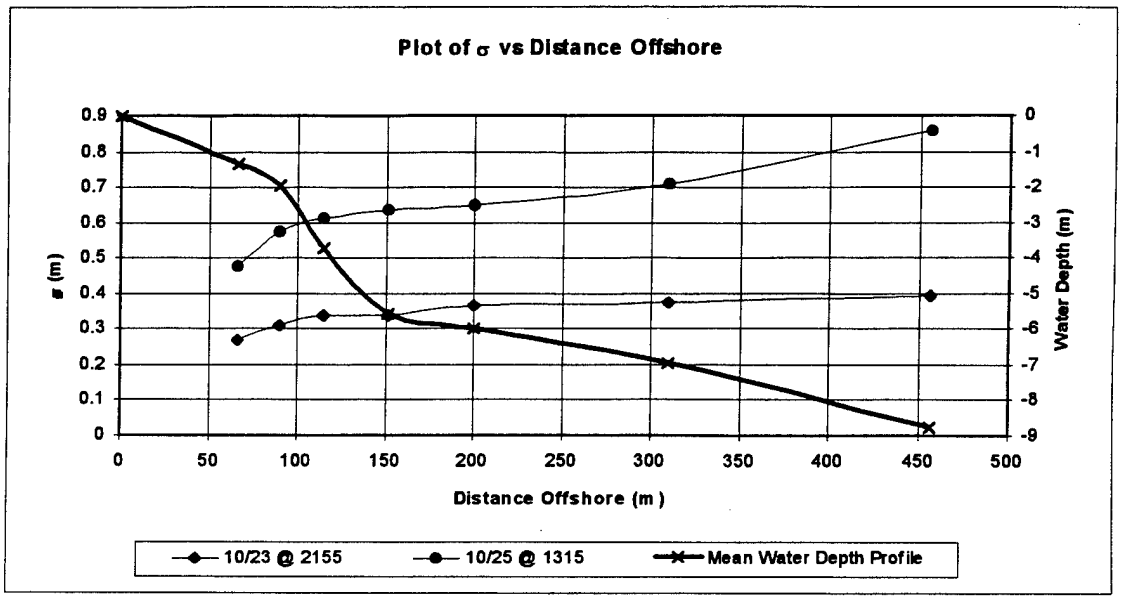

Figure 5.1 Spatial Comparison of σ at Mild and Severe Sea Conditions

The trends evident in Figure 5.2 reinforce the analysis done for the two cases in Figure 5.1. The upper bounds of the discrete data represent the severe sea conditions while the lower bounds represents the mild sea conditions.

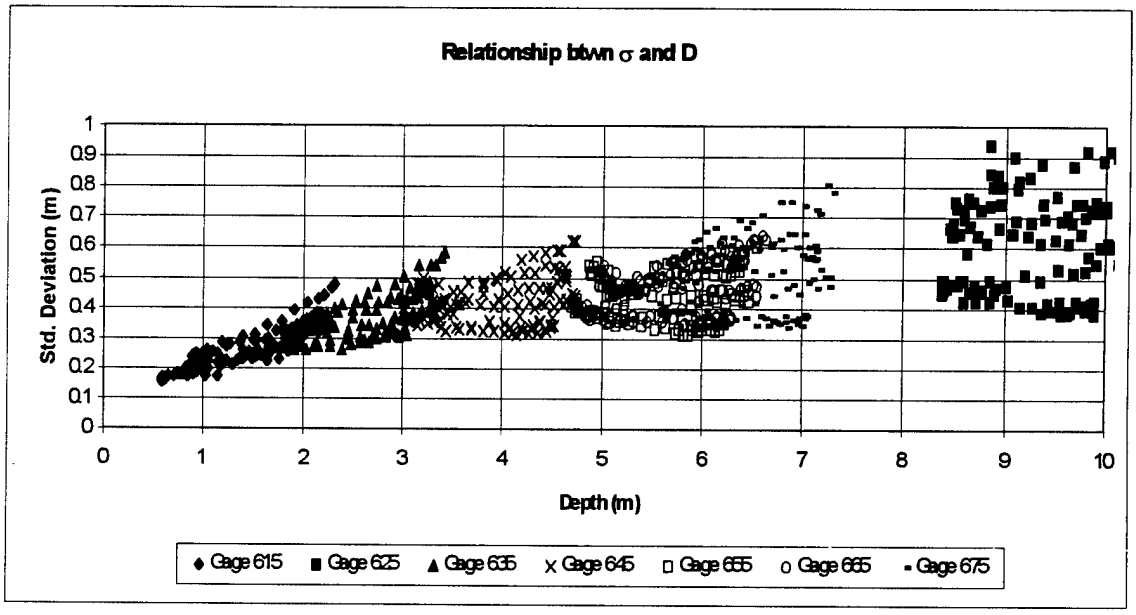

Figure 5.2 All σ Data Plotted as a Function of Water Depth

It can also be inferred from Figure 5.1 and Figure 5.2 that as the sea state becomes milder, the waves' standard deviation approaches a constant value and hence the sea severity approaches a constant before decreasing towards the origin.

In the absence of elaborate wave data, the value for σ can be readily determined with a knowledge of the local and breaking wave heights and the relative water depth, defined by $\frac{d}{gT^2}$, where g = gravitational constant and T = wave period, using a method such as stream function theory (Dean 1974). To ensure the use of accurate wave height values in applying the stream function theory, nonlinear shoaling methods should be used in finite water depths to determine the breaking and local wave heights.

5.2 Non-Gaussian PDF Parameter Analysis

The non-Gaussian probability density function parameters, a, μ_* and σ_*, will be analyzed in non-dimensional form spatially as a function of distance offshore, against each other in non-dimensional form, and with $a\sigma$ as a function of σ/d. The first analysis of the non-Gaussian probability density function parameters will involve comparing the non-dimensional parameters against the distance the gage was located offshore. This will provide a spatial orientation of the parameters which will disregard any local fluctuations in water depth due to tidal cycle of storm surge. The results are shown in Figures 5.3-5.5.

5.2.1 Spatial Analysis of Parameters

All three parameters shown in Figures 5.3-5.5 appear to gradually increase in absolute magnitude until approximately 150 meters to 175 meters offshore. The mild condition represented by 10/23 @ 2155 consistently yields lower values when compared with the more severe sea condition on 10/25 @ 1315. As the sea condition becomes more mild, the wave profile resembles the normal distribution. When the wave profile represents exactly the normal distribution, "a" equals zero and σ_* equals σ. It can be seen

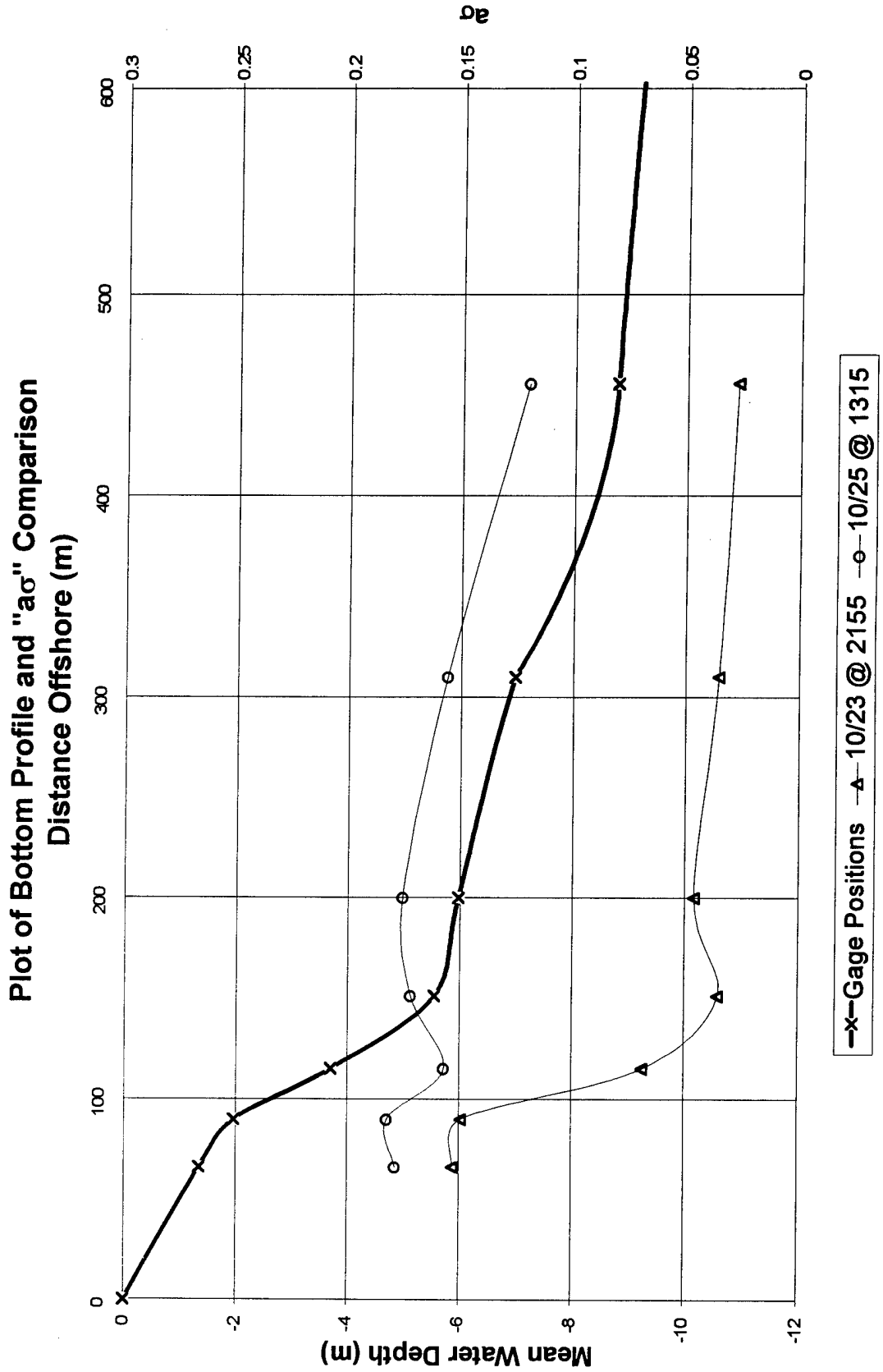

Figure 5.3 Spatial Comparison of aσ at Mild and Severe Sea Conditions

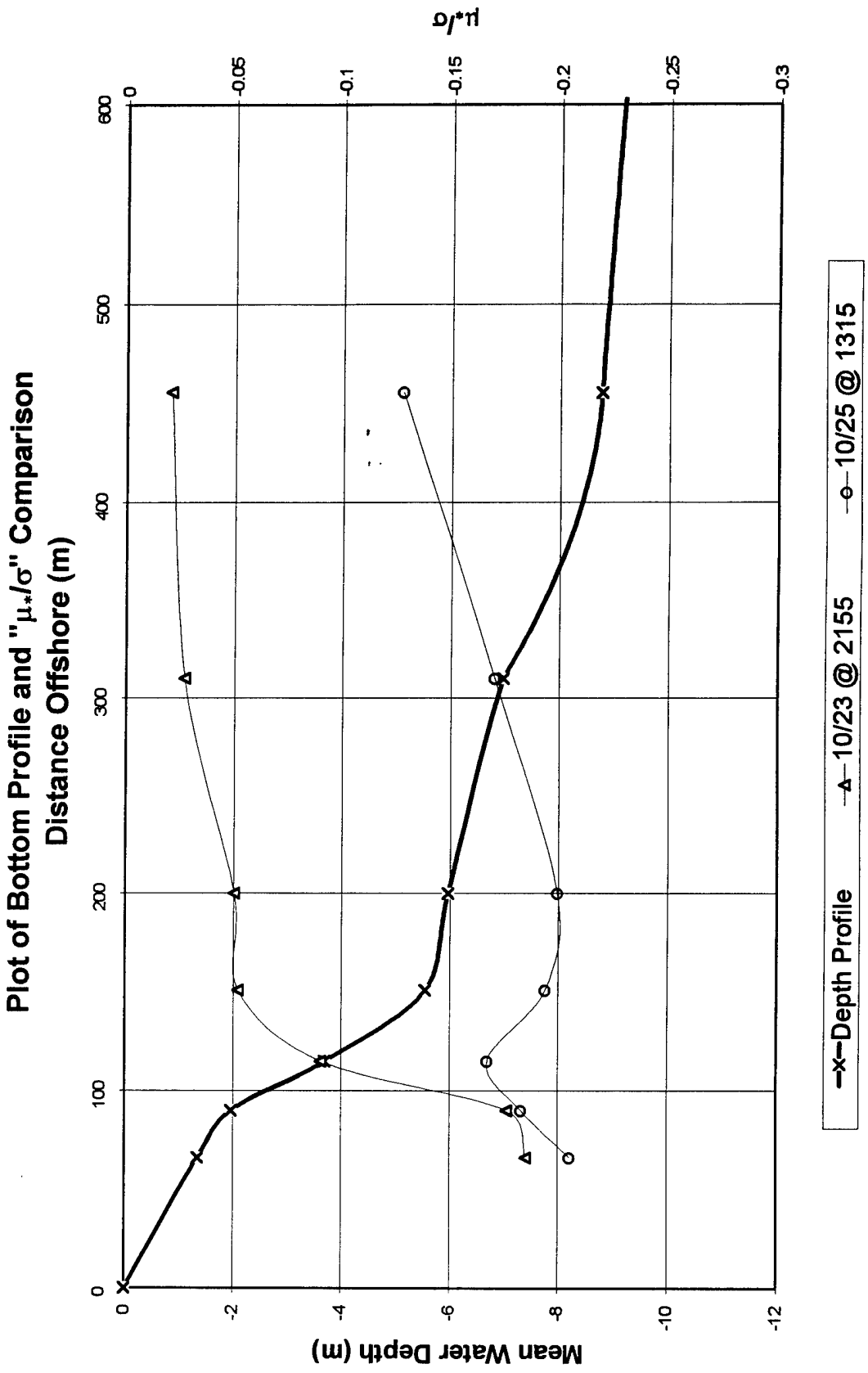

Figure 5.4 Spatial Comparison of μ*/σ at Mild and Severe Sea Conditions

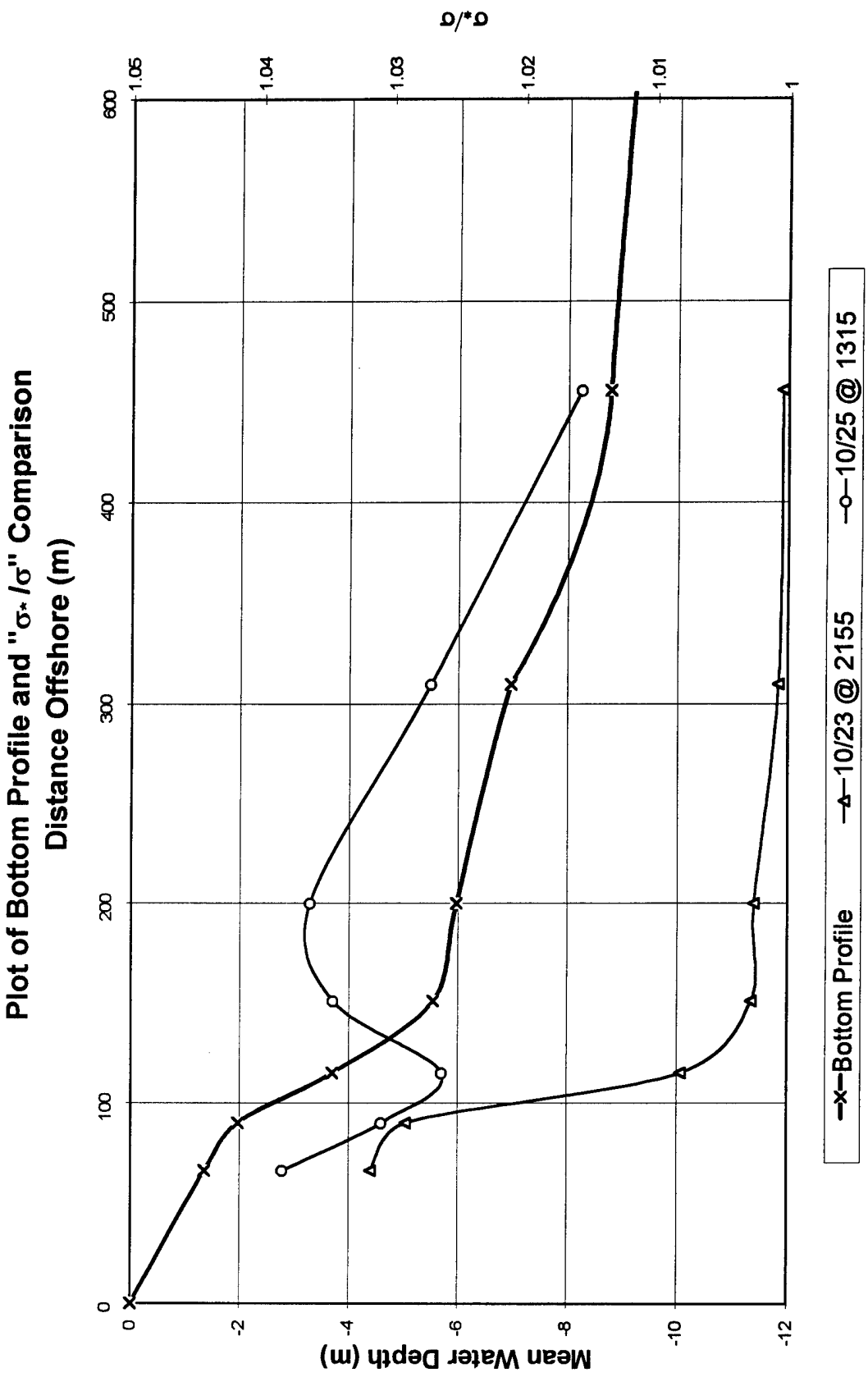

Figure 5.5 Spatial Comparison of σ*/σ at Mild and Severe Sea Conditions

from Figures 5.3 and 5.5 that as approaches zero under mild conditions and s_*/s approaches one. Figure 5.4 shows that m_*/s approaches zero under these same conditions which is also consistent with the theoretical limit of the non-Gaussian probability density function.

There is also a significant perturbation evident in Figures 5.3-5.5 around 150 meters offshore. The mild sea condition shows this abrupt change occurring seaward when compared with its location under severe sea conditions and the perturbation is more pronounced in the severe sea condition case. In general, all trends analyzed for the non-dimensional parameter, m_*/s, are almost identical results to those found for as and s_*/s but in the mirror image. This is due to the fact that the value of m_* is negative. The negative sign is supported by the theory used to develop the probability density functions' three governing equations.

The next spatial analysis will consist of comparing the non-dimensional parameters with water depth. This comparison will be sensitive to any influence of local depth changes occurring from tidal cycles and/or storm surges. Figures 5.6 - 5.8 show the results of this analysis.

The trends from this analysis are the same as those determined by Figures 5.3-5.5. Due to the difference in scale of the abscissa the curves based on water depth appear to show much smoother transitions. Figures 5.6-5.8 include two additional cases representing intermediate sea conditions between those represented by 10/23 @ 2155 and 10/25 @ 1315. These two additional cases approximate the trends displayed by the mild sea condition of 10/23 @ 2155. This is consistent with the data and time of these cases since they occurred prior to the severe storm so the sea condition was not yet impacted significantly.

As was discussed earlier, in the deeper water conditions all three parameters tend to show convergence towards their respective values for a Gaussian wave profile. In extremely shallow water conditions, the parameters also tend to converge towards a

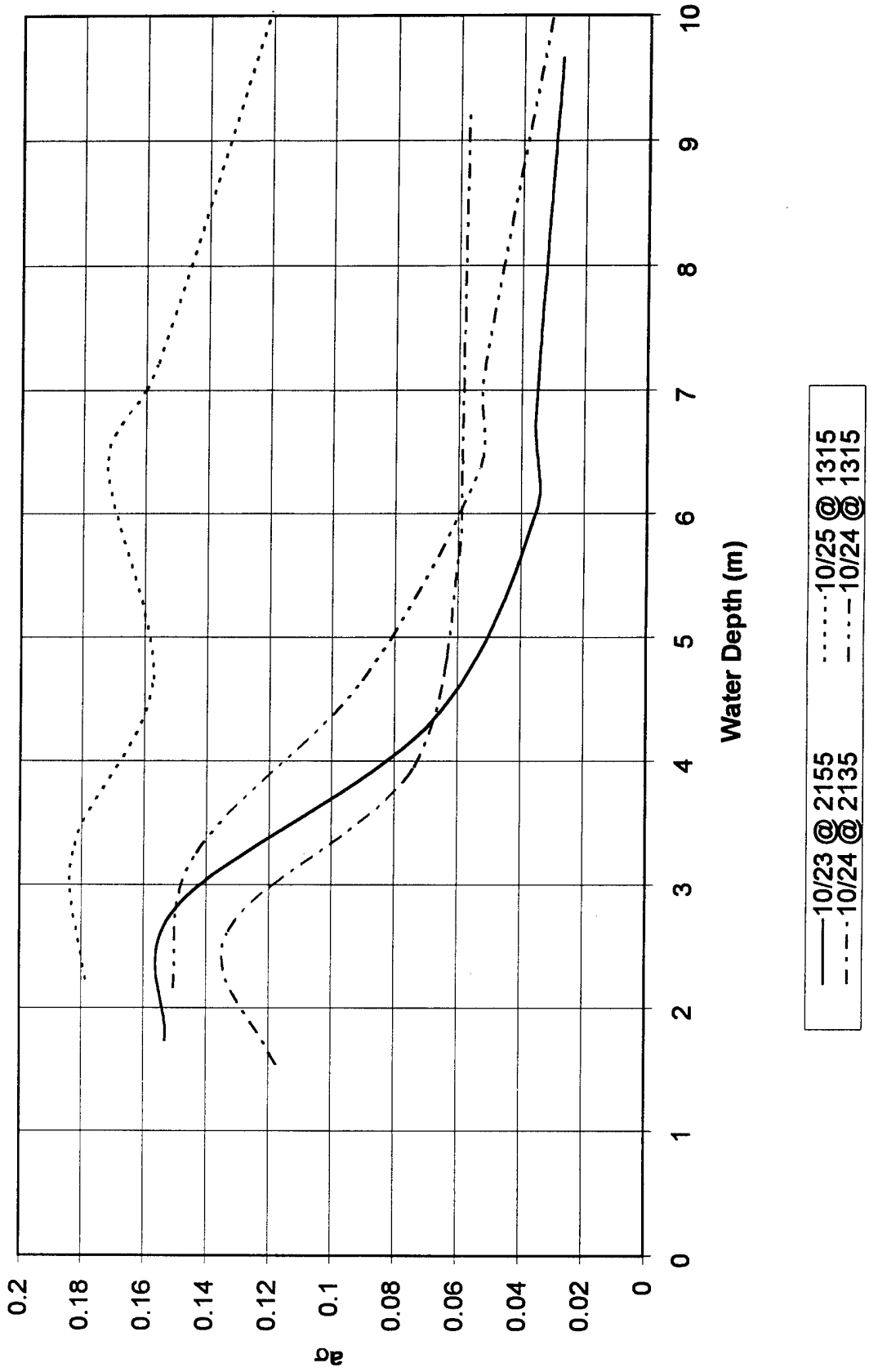

Figure 5.6 aσ as a Function of Water Depth

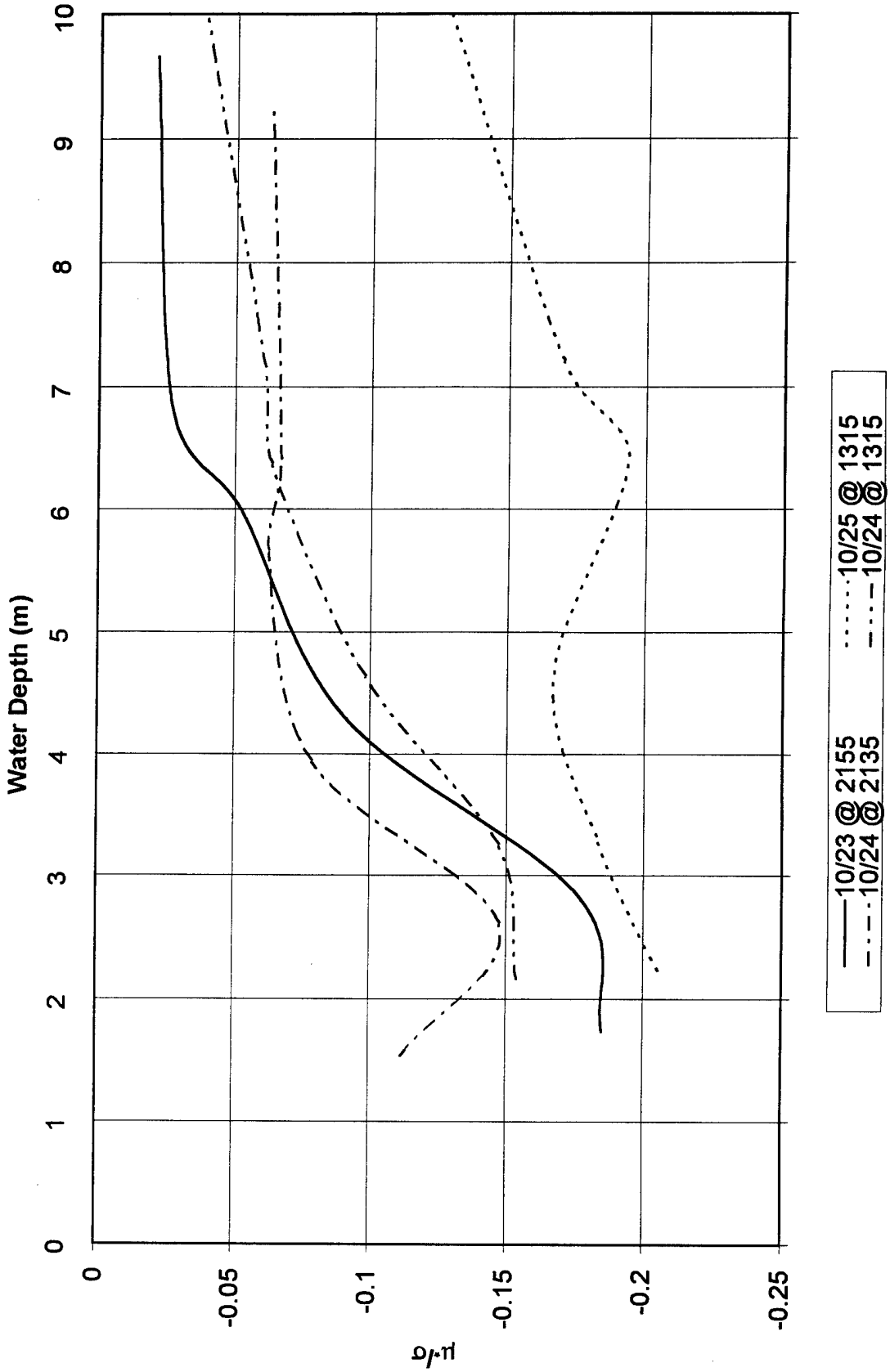

Figure 5.7 μ./σ as a Function of Water Depth

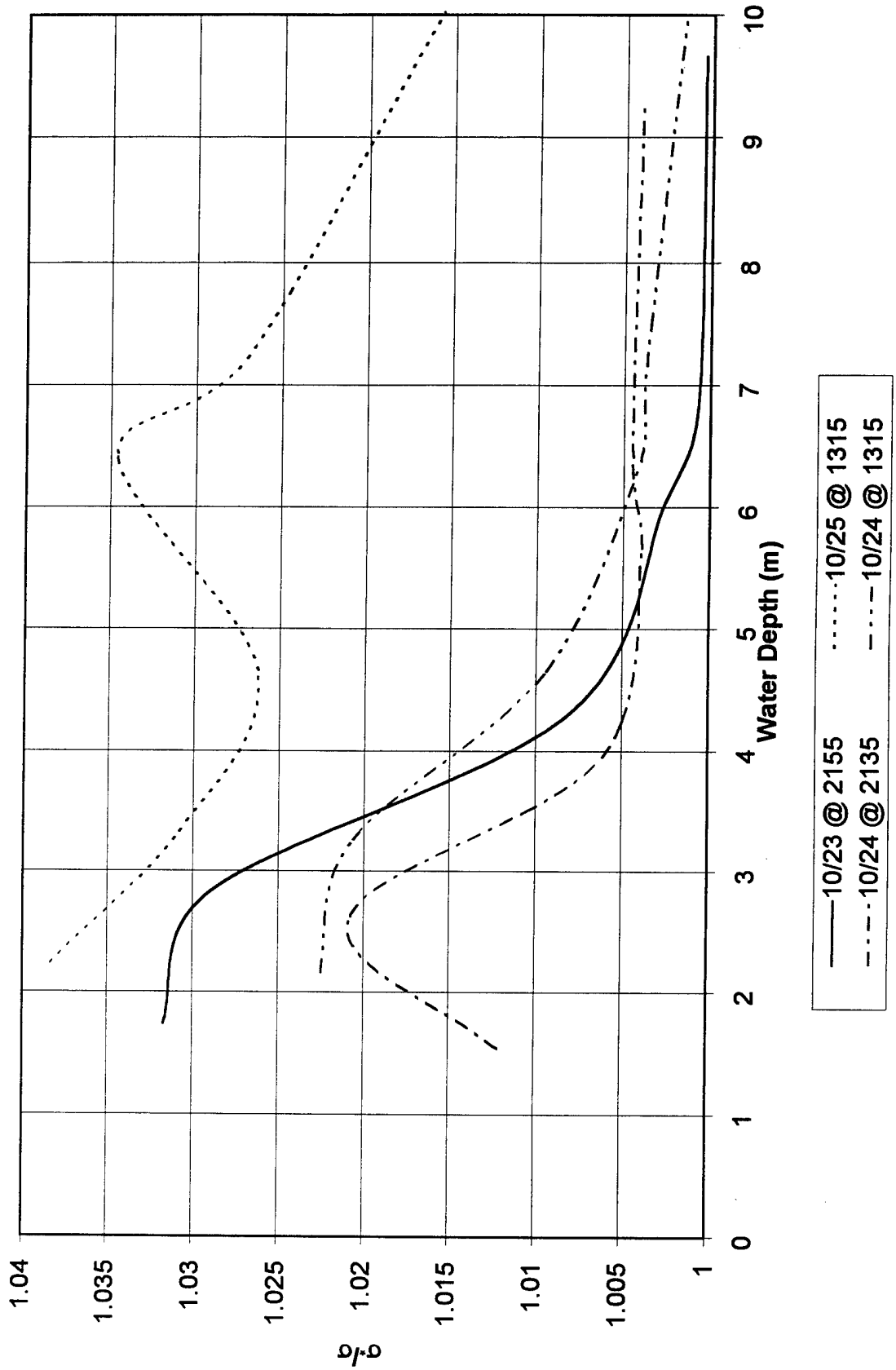

Figure 5.8 σ_t/σ as a Function of Water Depth

constant value which is different depending on the sea condition. For the milder sea conditions, the parameters tend to converge to the values shown in Table 5.1.

Table 5.1 General Shallow Water Limits of Parameters

Non-Dimensional Parameter	Mild - 10/23 @ 2155	Severe - 10/25 @ 1315
$a\sigma$	0.15	0.18
μ_*/σ	-0.18	-0.22 to -0.25
σ_*/σ	1.033	1.04 to 1.045

When the separate plots for each non-dimensional parameter are compared in both spatial cases, it is apparent that similar trend descriptions fit all three parameters. For this reason, a closer analysis will be made among the three variables to determine if this similarity can be quantified. The next trend analysis consists of comparing the three parameters with each other.

5.2.2 Relationship Between the three non-dimensional parameters, $a\sigma$, μ_*/σ and σ_*/σ

As discussed earlier, the three non-dimensional parameters appear to be highly correlated with each other. A closer look will be taken to see if specific relations can be developed connecting the three non-dimensional parameters together. Figure 5.9 and Figure 5.10 show plots of the raw data representing μ_*/σ and σ_*/σ compared with $a\sigma$ respectively at the extreme water depth locations, gage 615 and gage 625.

All data sets from Gages 615 and 625 were plotted since they represent the shallowest and deepest gage locations. There are very definite relationships which hold constant between the extreme range of water depths and sea conditions, that link $a\sigma$ to μ_*/σ and σ_*/σ. The functional relationship can be determined only after considering all

the data points from all water depth and sea severity conditions to ensure it remains consistently valid. A deterministic relationship between these non-dimensional parameters is a topic of active research.

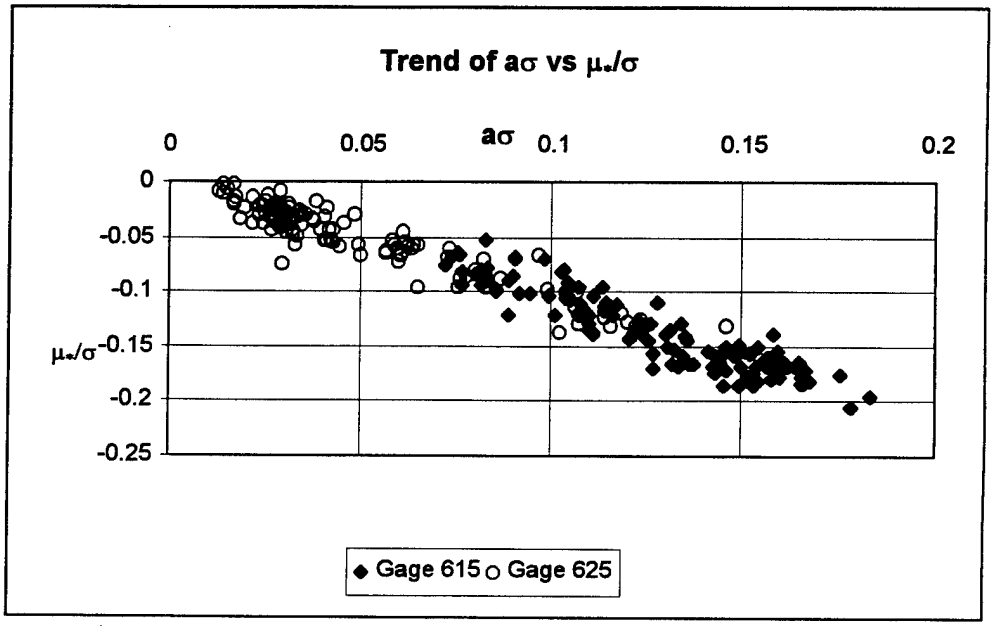

Figure 5.9 Plot of μ_*/σ as a function of $a\sigma$ for Gages 615 and 625

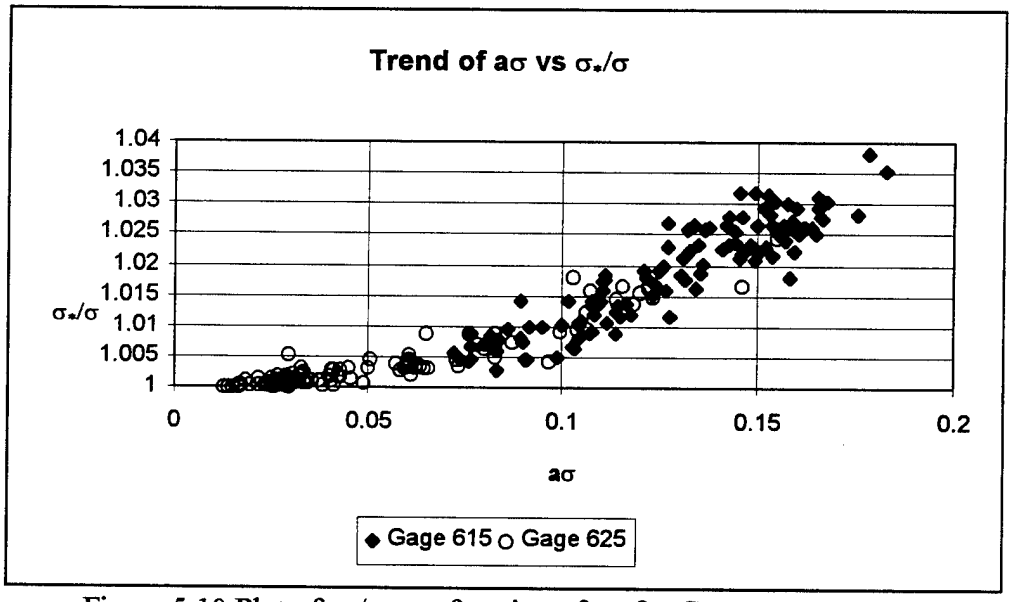

Figure 5.10 Plot of σ_*/σ as a function of $a\sigma$ for Gages 615 and 625

5.2.3 Relationship Between $a\sigma$ and σ/d

Based on the apparent correlation between the parameters of the non-Gaussian probability density function, $a\sigma$ will be used to represent the general trends of the other two parameters when plotted as a function of σ/d. This relationship is provided in Figure 5.11 to demonstrate general trends between the wave $a\sigma$, and the local environment represented in terms of sea severity/water depth in non-dimensional form. The lower values of σ/d correspond to the deeper gage locations and the trend is for these values to approach the values defined by wave profiles having a normal distribution. This plot also reinforces the analysis done in Chapter 4 which determined the boundary values of the Gaussian distribution. At $\sigma/d = 0.06$, the $a\sigma$ values appear to begin converging towards the Gaussian limit located at the origin of Figure 5.11.

The higher values of σ/d represent the shallower water depths. It appears that at these values $a\sigma$ tends to approach a finite asymptotic limit. This is consistent with the findings from the spatial analysis figures. In between these two limits of Figure 5.11 there is a depression in the severe sea condition case. This phenomenon must be analyzed more thoroughly to ascertain a reasonable explanation for its existence and will be the subject of a later study.

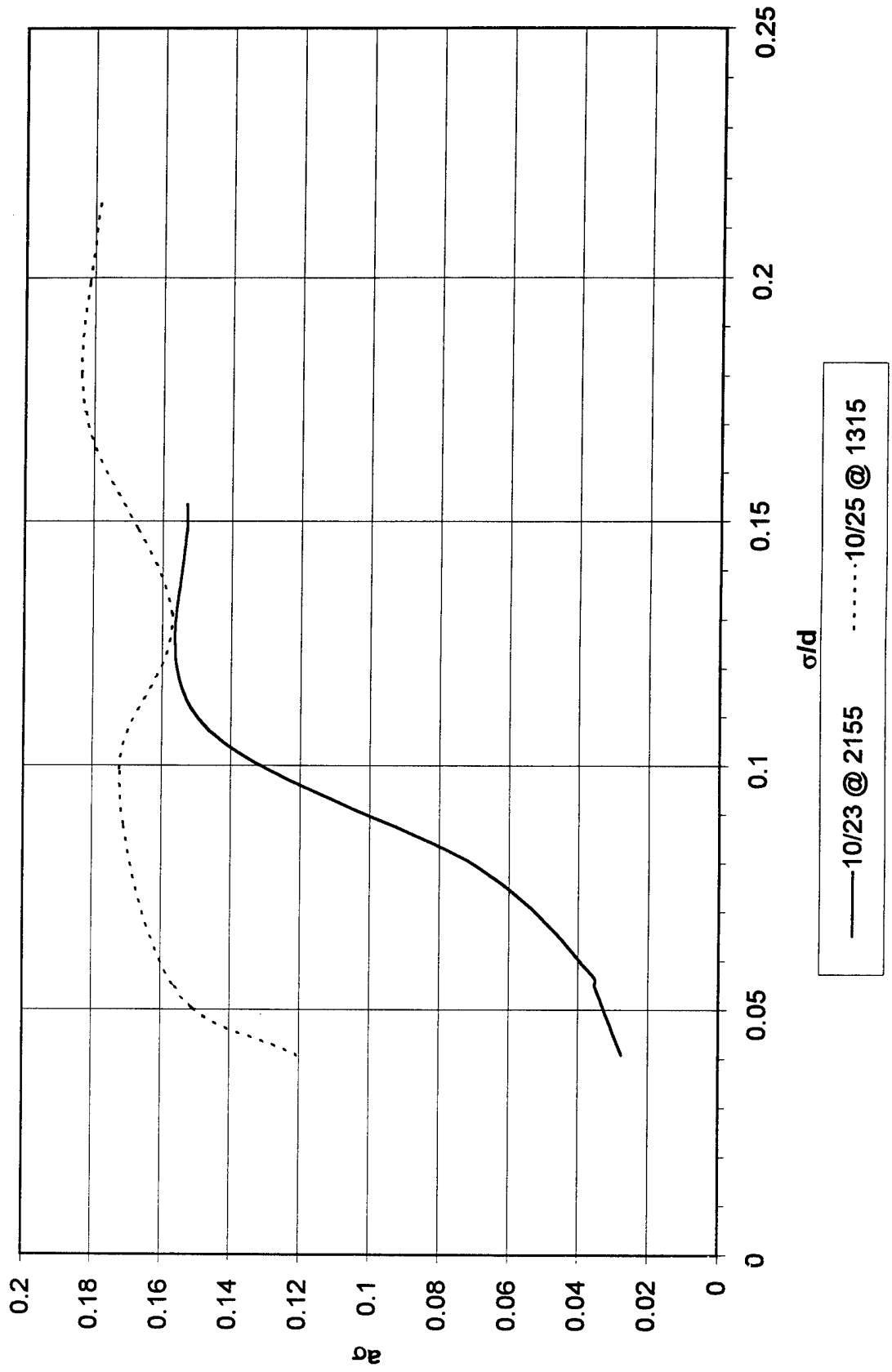

Figure 5.11 Plot of aσ as a Function of σ/d for Mild and Severe Sea Conditions

CHAPTER 6
SUMMARY AND CONCLUSIONS

It is shown, based on the results of this study, that wind generated waves exhibit significant changes in their profile forms as they propagate into finite water depths. The actual nature of this transformation has been a subject that has not been covered in any significant detail. The unique wave data records collected during the ARSLOE Project of 1980 enabled a detailed study on this topic to be produced.

One objective of this study was to verify the applicability of the non-Gaussian probability density function developed by Ochi and Ahn (1994b) defined as

$$f(x) = \frac{1}{\sqrt{2\pi}\sigma_*}\exp\left[-\frac{1}{2(\gamma a\sigma_*)^2}(1-\gamma a\mu_* - \exp(-\gamma a x))^2 - \gamma a x\right]$$

$$\text{where, } \gamma = \begin{cases} 1.28 \, for: x \geq 0 \\ 3.00 \, for: x < 0 \end{cases}.$$

Through statistical analysis of the ARSLOE data, it has been confirmed that this probability density function can be used with confidence to represent wave profiles in finite water depths. It correlates very well with histogram data over an extensive range of sea conditions. The distribution of the wave profile in finite water depths shows a dependence on water depth and sea severity. In particular, as water depth decreases, the distribution becomes increasingly non-Gaussian. Also, as sea severity increases the same trend occurs.

With the applicability of the probability density function verified, an analysis of the boundary condition where the wave profile can no longer be considered Gaussian was conducted. A general relationship has been proven to exist between the largest significant wave height and the local water depth where the wave profile can still be considered

Gaussian. This relationship is defined as $\frac{H_s}{d} = 0.24$ or $\frac{\sigma}{d} = 0.06$. Both forms of this relationship are identical since the significant wave height, H_S is defined as four times the standard deviation, σ, in deep water conditions. This relationship has been verified using three different approaches with each yielding similar results. In shallower water conditions, this boundary, defining the transition from Gaussian to non-Gaussian wave profiles, appears to shows a dependence on beach slope. This is a qualitative observation from the present study and additional research must be done to quantify this finding. This dependence on beach slope may be similar to the influence of beach slope on breaking waves. The linear result defined by this study is akin to the earliest breaking criterion based on Solitary Wave Theory.

At present, the only way this probability density function can be defined is through knowledge of statistical properties of the wave field of interest. In particular, the mean, variance and third moment of the wave profile must be known. This requires that wave profile data be obtained in order to evaluate the parameters of the probability density function.

Another objective of this study was to determine relationships linking the parameters of the probability density function to local field conditions. If the wave profile statistics can be defined in terms of local environmental conditions such as sea state and water depth, the probability density function can be defined without wave data. This study has revealed qualitative trends between the parameters of the probability density function and local field conditions based on the extensive data complied from ARSLOE. From these qualitative trends, it is evident that the specific relationships between the parameters and environmental conditions are complex and may require consideration of additional parameters besides sea severity, σ, and water depth. The pursuit of a functional relationship between the parameters and the local environment continues to be a topic of considerable interest and active research.

APPENDIX
COMPARISON OF ORIGINAL AND SMOOTHED "a" VALUES

It can be seen that the nonlinearity parameter, "a" is characterized by a significant amount of local flucuations superimposed on the overall trend of the parmeter. Based on the definition of "a" as a nonlinearity parameter used to describe the probability density function of a wave profile, these small flucuations can be smoothed without any noticable loss of accuracy. It is highly unlikely that the probability density function of a wave profile changes so sporadically over such short periods of time as indicated by the minor variations of "a". There was not any one smoothing technique that was used in the smoothing of "a" at all gage positions. Instead, several smoothing techniques were evaluated and the technique which produced the lowest mean absolute deviation (MAD) was the technique used for that particular gage position.

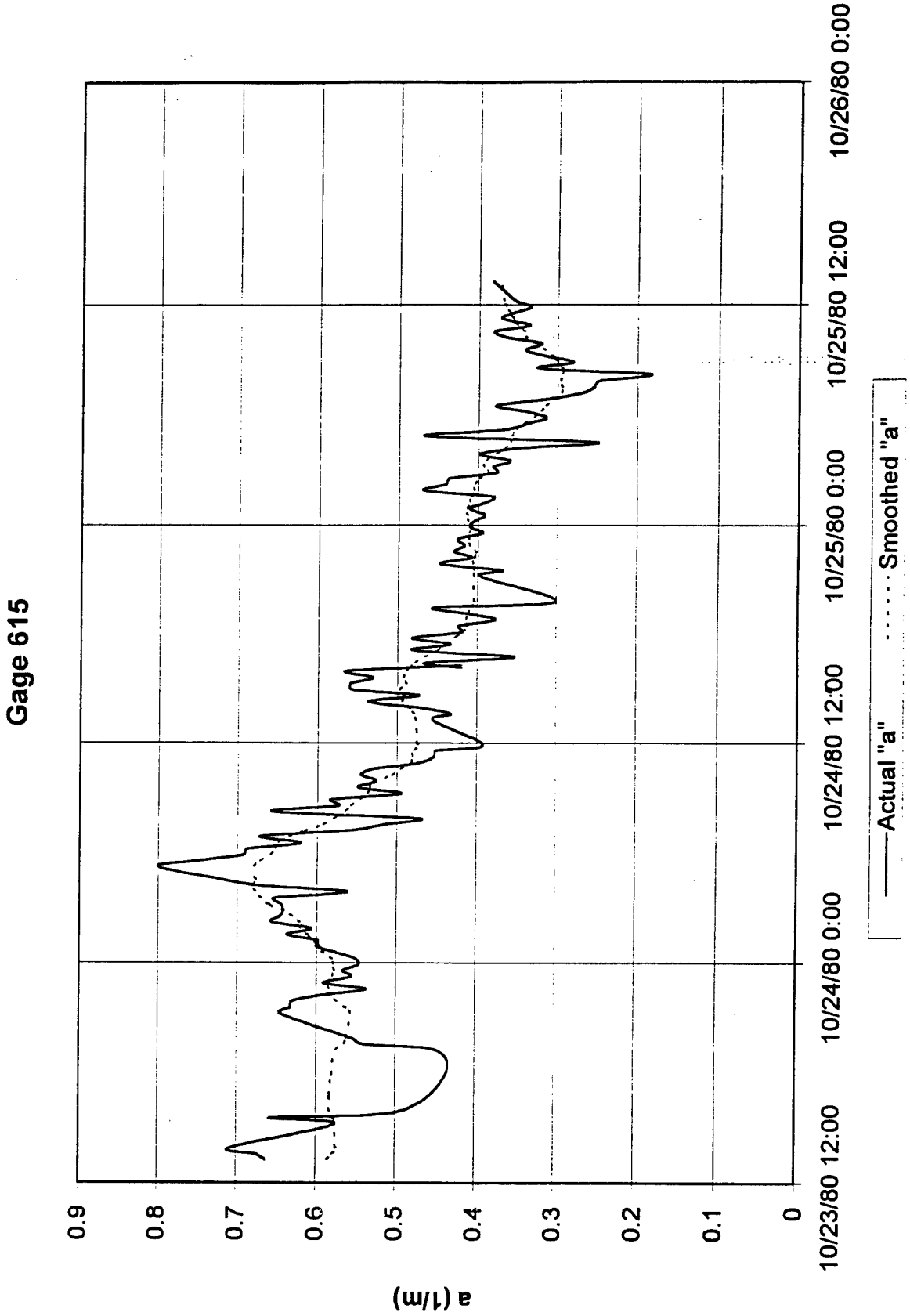

Figure A.1. Plot of Gage 615 Original and Smoothed "a" Values

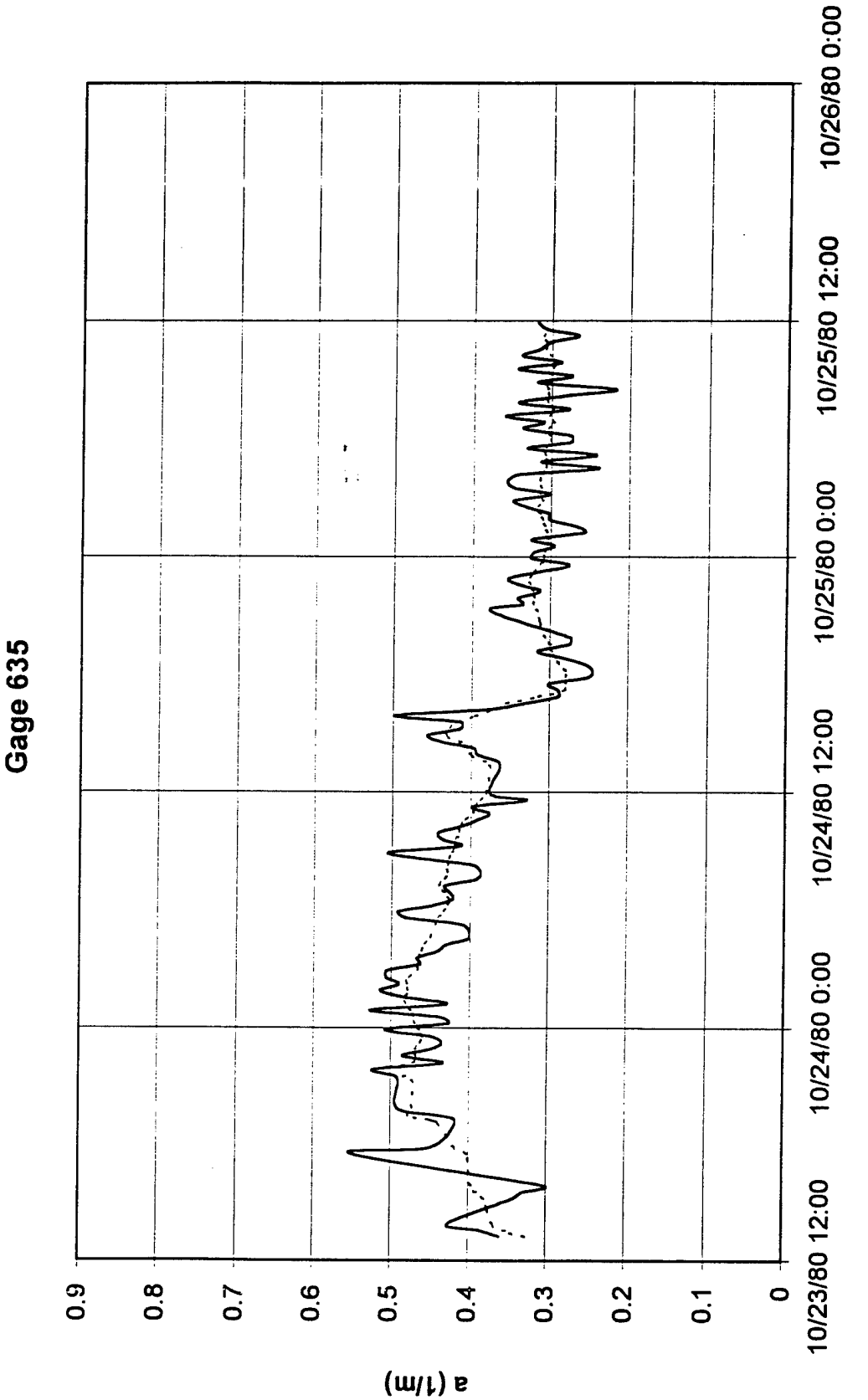

Figure A.2. Plot of Gage 635 Original and Smoothed "a" Values

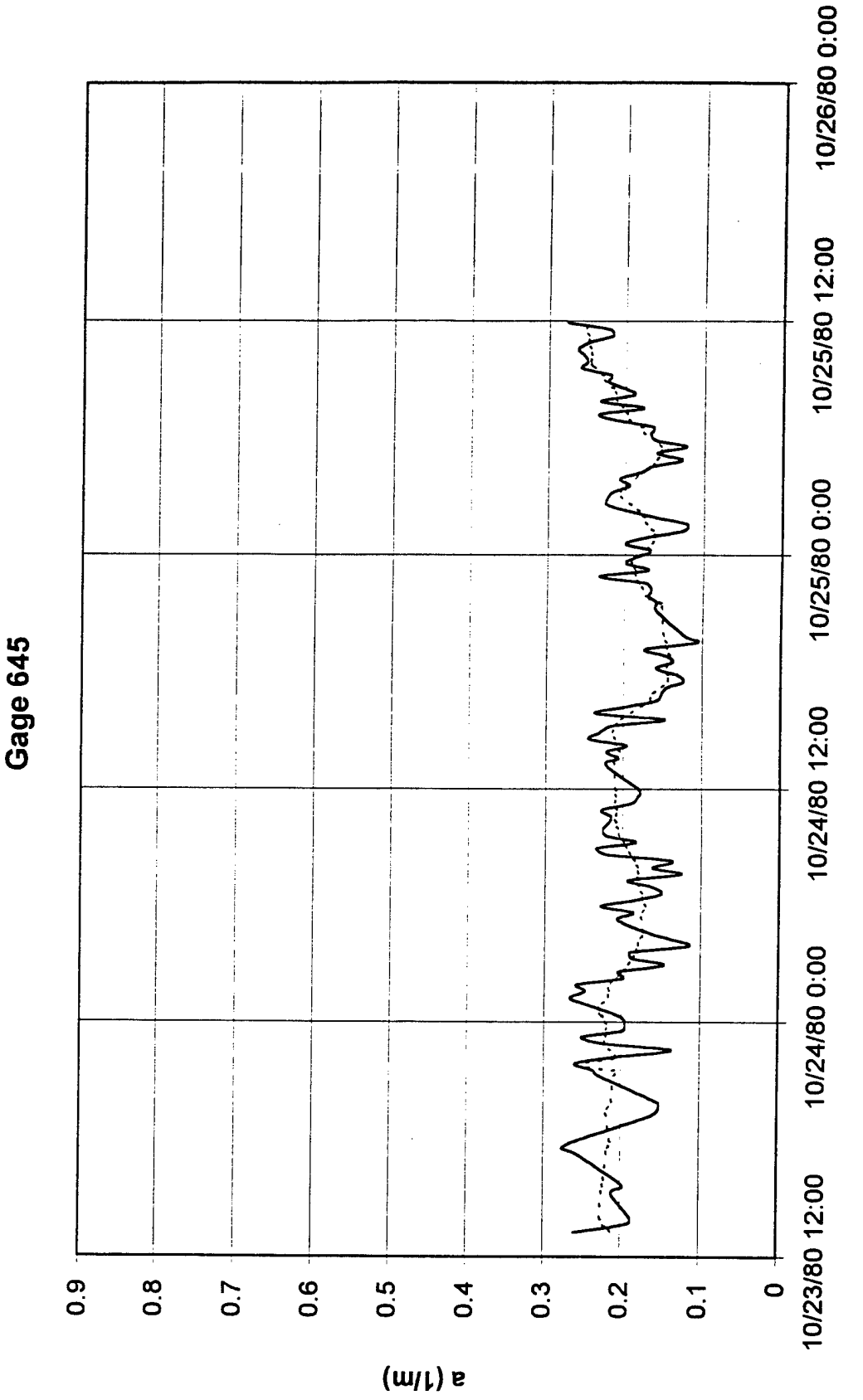

Figure A.3. Plot of Gage 645 Original and Smoothed "a" Values

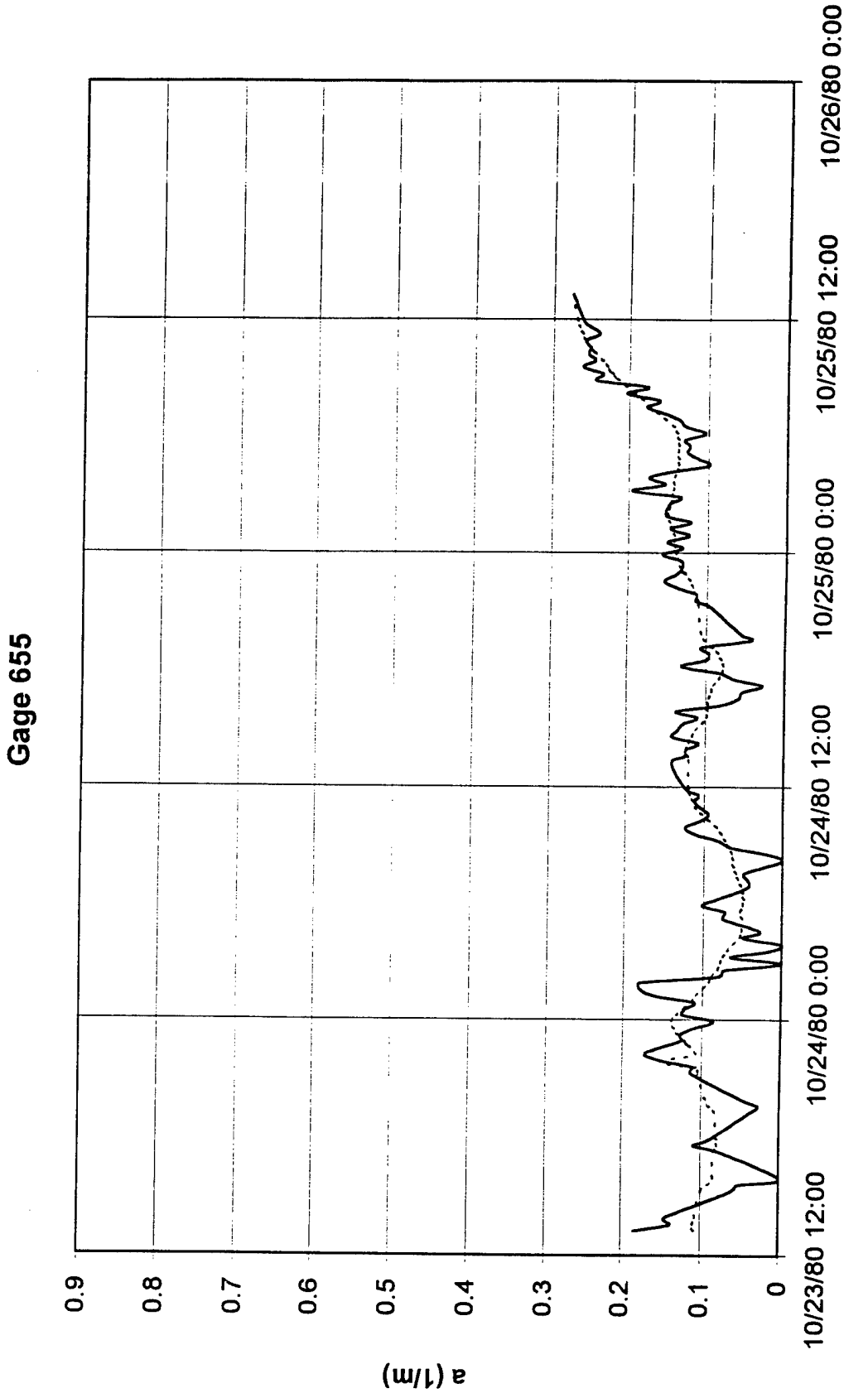

Figure A.4. Plot of Gage 655 Original and Smoothed "a" Values

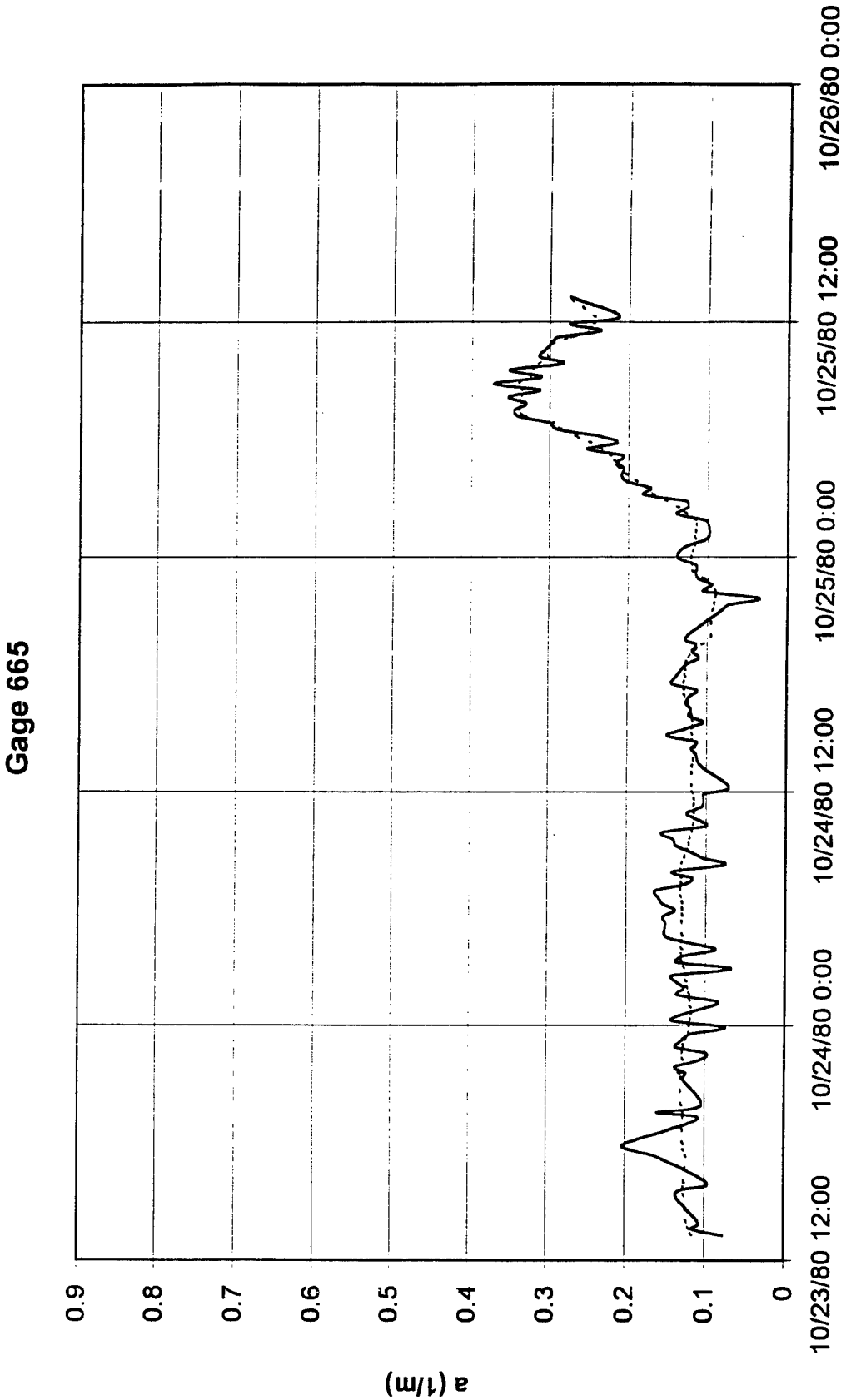

Figure A.5. Plot of Gage 665 Original and Smoothed "a" Values

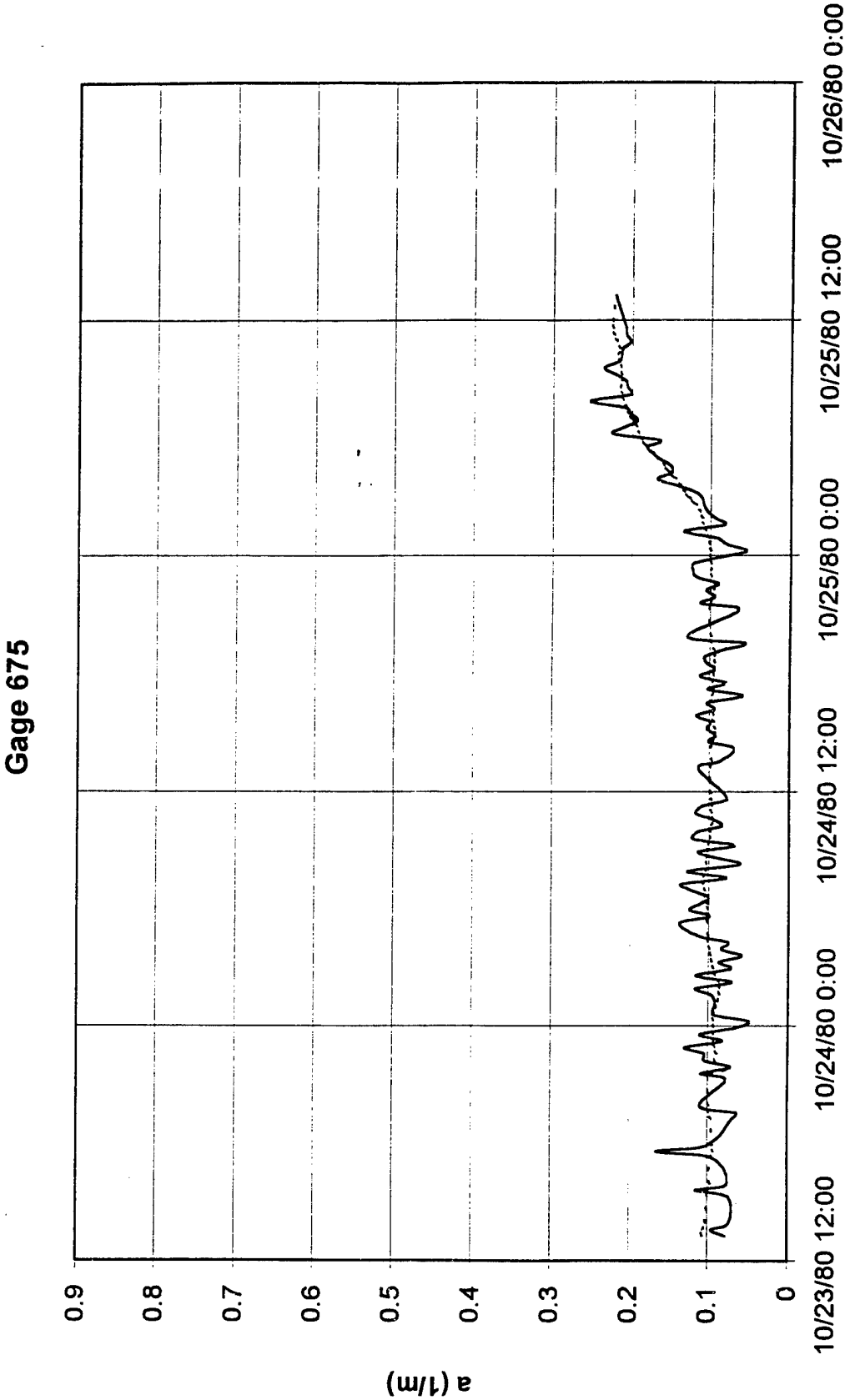

Figure A.6. Plot of Gage 675 Original and Smoothed "a" Values

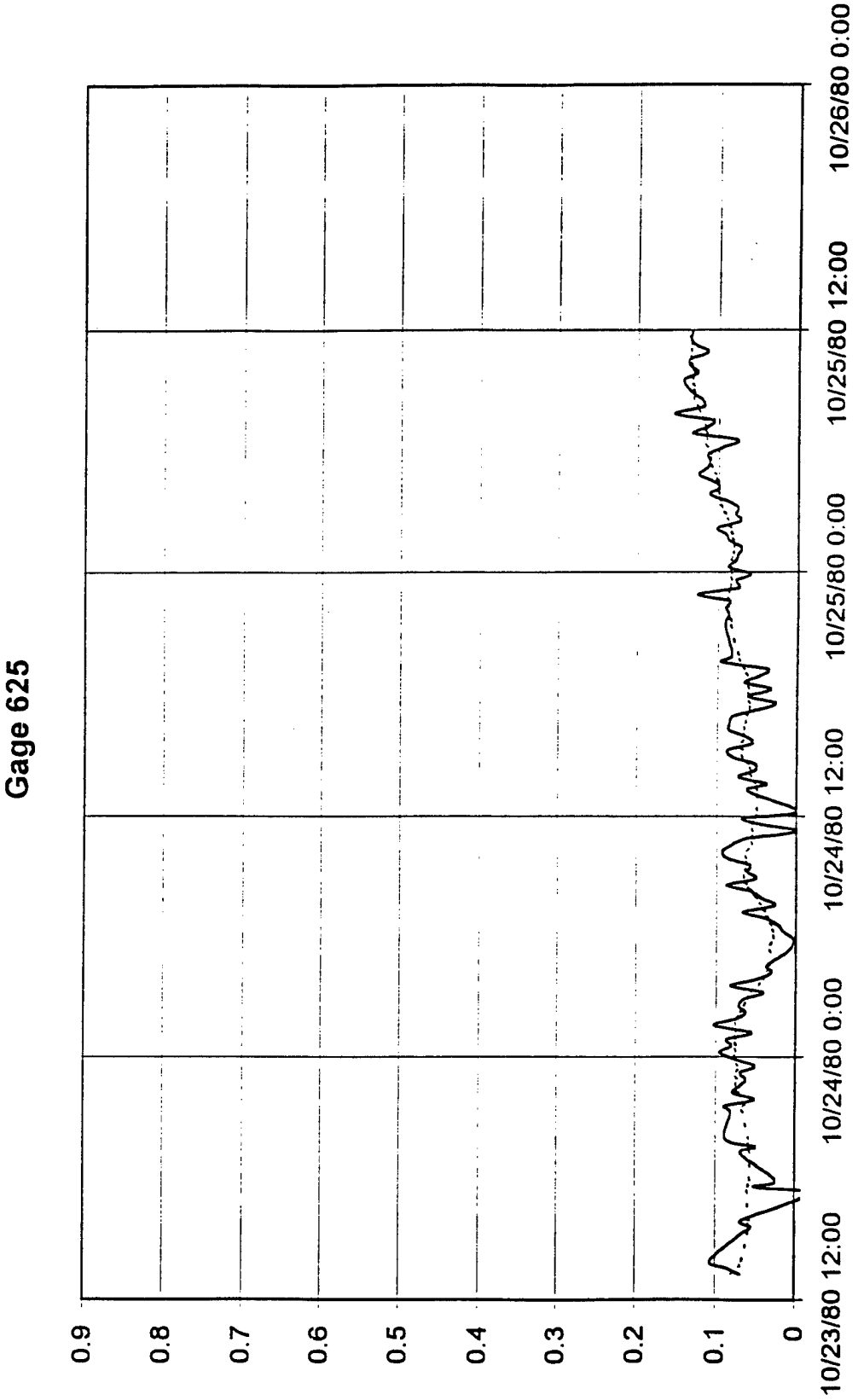

Figure A.7. Plot of Gage 625 Original and Smoothed "a" Values

LIST OF REFERENCES

Bitner, E.M. (1980), "Nonlinear Effect of the Statistical Model of Shallow Water Wind Waves," Applied Ocean Resources Vol. 2,No.2, pp. 63-73.

Dean, R.G. (1974), "Evaluation and Development of Water Wave Theories for Engineering Application," Vols. 1 and 2, Spec. Rep. 1, U.S. Army, Coastal Engineering Research Center, Fort Belvoir, VA.

Doering, J. C., Donelan, M. A. (1993), "The Joint Distribution of Heights and Periods of Shoaling Waves," Journal Geophy. Res., Vol 98, No. C7, pp. 12,543-12,555.

Huang, N.E., Long, S.R., Tung, G.G. and Yuan, Y. (1983), "A Non-Gaussian Statistical Model for Surface Elevation of Nonlinear Random Waves," Journal Geophy. Res., Vol.88, No.C12, pp.7597-7606.

Kac, M. and Siegert, A.J.F. (1947), "On the Theory of Noise in Radio Receivers with Square Law Detectors," J. Applied Physics, Vol.8, pp.383-397.

Langley, R.S. (1987), "A Statistical Analysis of Non-Linear Random Waves," Ocean Engineering, Vol.14, No.5, pp.389-407.

Longuet-Higgins, M.S. (1963), "The Effect of Non-Linearities on Statistical Distributions in the Theory of Sea Waves," J. Fluid Mech., Vol.17, Part 3, pp. 459-480.

Ochi, M.K. and Wang, W.C. (1984), "Non-Gaussian Characteristics of Coastal Waves," Proc. 19th Coastal Eng. Conf., Vol.1, pp. 836-854.

Ochi, M.K. and Ahn, K. (1994a), "Probability Distribution Applicable to Non-Gaussian Random Process," J. Probabilistic Eng. Mech., Vol. 9, pp.255-264.

Ochi, M.K. and Ahn, K. (1994b), "Non-Gaussian Probability Distribution of Coastal Waves," Proc. 24th Coastal Engineering Conf., Vol.1, pp. 482-496.

Tayfun, M.A. (1980), "Narrow-Band Non-Linear Sea Waves," J. Geophy. Res. Vol.85, No.C3, pp.1548-1552.

Thornton, E.B. and Guza, R.T.(1983), "Transformation of Wave Height Distribution," J. Geophy. Res., Vol.88, No.C10, pp. 5925-5938.

Weggel, J.R. (1972), "Maximum Breaker Height," J. Waterways, Harbors Coastal Eng. Div., ASCE, Vol. 98, No.WW4, pp. 1245-1267.

BIOGRAPHICAL SKETCH

The author was born on September third, 1966, in Albany, New York. His affinity toward the ocean was evident in high school. Upon graduation from high school, he attended the U. S. Naval Academy and graduated in 1988 with a B.S. degree in Ocean Engineering. He began his naval career as a Navy Diver serving on a minesweeper. In October 1991, he transferred into the U. S. Navy Civil Engineer Corps.

He arrived in Gainesville in January 1995 to begin graduate work in the field of coastal engineering under Dr. Michel K. Ochi. A short one and one-half years later, in May 1996, he is on his way to Panama City, Florida, to serve as the Engineering Officer at the Navy Experimental Diving Unit.